Performance Analysis of Vehicular Device-to-Device Underlay Communication

Nan Cheng, *Member, IEEE,* Haibo Zhou, *Student Member, IEEE,* Lei Lei, *Member, IEEE,* Ning Zhang, *Student Member, IEEE,* Yi Zhou, *Member, IEEE,* Xuemin (Sherman) Shen, *Fellow, IEEE,* Fan Bai, *Fellow, IEEE*

Abstract—The demand for vehicular mobile data services has increased exponentially, which necessitates alternative data pipes for vehicular users other than the cellular network and dedicated short-range communication (DSRC). In this paper, we study the performance of underlaid vehicular device-to-device (V-D2D) communications, where the cellular uplink resources are reused by V-D2D communications, considering the characteristics of the vehicular network. Specifically, we model the considered urban area by a grid-like street layout, with non-homogeneous distribution of vehicle density. We then propose to employ a joint power control and mode selection scheme for the V-D2D communications. In the scheme, we use channel inversion to control the transmit power, in order to determine transmit power based on pathloss rather than instantaneous channel state information, and avoid severe interference due to excessively large transmit power; the transmission mode is selected based on the biased channel quality, where D2D mode is chosen when the biased D2D link quality is no worse than the cellular uplink quality. Under the proposed scheme, two performance metrics of V-D2D underlaid cellular networks, SINR outage probability and link/network throughput, are theoretically analyzed. Simulation results validate our analysis, and show the impacts of design parameters on the network performance.

I. INTRODUCTION

Future vehicles are expected to be not only faster and safer, but also greener, and more comfortable and entertaining for the passengers. One major technology to meet this expectation is VehiculAr NETworks (VANETs): automobiles are equipped with wireless communication capabilities, enabling them to communicate with each other, and with other networks, such as the Internet. VANETs can facilitate a variety of applications, such as safety applications (e.g., collision warning and lane change warning), road traffic management, and vehicular mobile data services (e.g., content uploading and sharing, mobile video streaming, online gaming) [1], [2]. The soaring number of connected cars with Internet access, along with the emerging vehicular mobile data services will altogether impose stringent requirements towards its enabling technology solutions. For example, the update of smart vehicle software

N. Cheng, H. Zhou, N. Zhang, and X. Shen are with the Department of Electrical and Computer Engineering, University of Waterloo, 200 University Avenue West, Waterloo, ON N2L 3G1, Canada (e-mail:{n5cheng , n35zhang, sshen}@uwaterloo.ca).

L. Lei is with State Key Laboratory of Rail Traffic Control and Safety and the School of Electronic and Information Engineering, Beijing Jiaotong University, Beijing 100044, P.R. China (e-mail:leil@bjtu.edu.cn).

Y. Zhou (corresponding author) is with School of Computer and Information Engineering, Henan University, Kaifeng 475004, Henan, P.R. China (e-mail:zhouyi@henu.edu.cn).

F. Bai is with the ECI Lab, General Motors Corporation, Warren, MI 48092 USA (e-mail: fan.bai@gm.com).

and upload of user generated data needs a high data rate, while the mobile high-quality video streaming requires low communication delay, high data rates, and high reliability jointly.

Currently, cellular technologies and dedicated short-range communication (DSRC) are two main means for vehicular data services. Cellular access technology, such as Long-term Evolution (LTE), provides reliable and ubiquitous Internet access to vehicles, thanks to its well planned and widely available cellular infrastructure. Many car manufacturers have chosen cellular technologies as their vehicular Internet access solutions (e.g., GM OnStar and BMW ConnectedDrive). However, the exponential growth of mobile data traffic makes cellular network straining to meet the growing demand of mobile data, resulting in an increasingly severe overload problem [3]. Based on a mobile data forecast from Cisco, the number of interconnected mobile devices will exceed 11 billion in 2019, and the global mobile data will exceed 20 exabytes per month by the same time [4]. It is fairly clear that simply using cellular networks for vehicular Internet access may only worsen the existing overload problem, further degrading the performance for both non-vehicular and vehicular users (VUs). In addition, the cost structure of cellular network could also put significant economic burden on the car manufacturers and car owners.

With specifically designed protocols and dedicated spectrum, DSRC also supports a rich variety of vehicular applications, including, but not limited to, safety applications, proximate file sharing, and Drive-Through Internet access [5]. However, when comparing to ever-growing mobile data demand, the bandwidth offered by DSRC solution is rather limited as well. This will be particularly worse in urban environments where there tends to have high vehicle density [6], [7]. Moreover, due to the contention-based channel access model, the performance of vehicular mobile data services can hardly be guaranteed as in the cellular-based technologies.

To address these issues, additional data pipes for VUs are desirable, which mitigate the congestion in cellular networks or in DSRC spectrum, and provide data services to vehicles with QoS guarantee. Device-to-device (D2D) communication is envisioned as a promising solution for next-generation vehicular communication system [8]. The basic tenet of D2D communications is that mobile users in proximity can communicate directly with each other on licensed cellular spectrum (or other spectrum bands) without traversing base stations or the cellular backhaul networks [9]–[11]. By utilizing the proximity of mobile users, concurrent transmissions can reuse the same spectrum band without severely interfering each

This article has been accepted for publication in a future issue of this journal, but has not been fully edited. Content may change prior to final publication. Citation information: DOI 10.1109/TVT.2016.2627582, IEEE Transactions on Vehicular Technology

2

other, which significantly enhances the spectrum efficiency. In addition to spectrum utilization, vehicular D2D (V-D2D) communication can provide more benefits. Comparing to the transmitter-BS-receiver two-hop cellular transmission, V-D2D communication offers much shorter communication latency due to the one-hop proximate transmission, which facilitates delay-sensitive vehicular data services. Moreover, unlike distributed DSRC, V-D2D communications are controlled by the (centralized) cellular networks, in both control plane functions (e.g., connection setup and maintenance) and data plane functions (e.g., resource allocation). Thus, a better performance is expected thanks to collision avoidance and careful interference mitigation. Also, varied QoS requirements, such as rates, can be satisfied by resource (sub-carrier) allocation mechanisms. Finally, D2D communications could be less expensive than conventional cellular communications because of its inherent nature of spectrum reuse [12].

Due to the advantages of the D2D technology, it is suitable for many vehicular use cases, and can enable novel location-based and peer-to-peer applications and services. For example, considering the huge number of connected smart cars (90% new cars in 2020), the update of smart cars software can put a significant burden on the cellular network, and cost a lot of money of car manufacturers and car owners. Thus, the software update package can be first downloaded by chosen vehicles, and exchanged among other vehicles by vehicular D2D (V-D2D) communications. In the process, the cellular network can apply efficient algorithms to choose downloading vehicles, assist pair devices to reduce delay, and allocate resources (sub-carriers) to mitigate interference, satisfy different QoS requirements, and optimize the performance. In this way, most of the traffic can be offloaded to local V-D2D transmissions, and thus much cellular bandwidth and money can be saved. Moreover, due to the loose delay requirement of software update, the vehicular delay tolerant network (VDTN) can be employed where the package can be disseminated in a store-carry-and-forward manner, which can further offload the cellular network and save the cost. Another type of data service is gaming and video/audio streaming among vehicular users, such as in the vehicular proximity social network [13]. Normally, these services are supported by DSRC or WiFi-direct communication, which may not satisfy the requirements due to the collisions and long device paring time. With V-D2D communication, such services can be better sustained due to cellular-controlled connection setup with shorter delay, and resource (sub-carrier) allocation which can support varied rates.

Somewhat to our surprise, we realize that there lacks a theoretical study that systematically investigates the performance of D2D communication for vehicular network scenarios. Indeed, this topic is a challenging research problem. First, unique mobility patterns of vehicles impact the network performance differently, when comparing to well-understood human mobility patterns. Second, the grid-like vehicular network topology degrades the spectrum reuse efficiency, since V-D2D communications only happen on roads. Last but not the least, the interference pattern is even more difficult to model than normal D2D communications where the spatial user distribution can be modeled by Poison point process (P.P.P.) [14].

To bridge this gap, in this paper, we establish a theoretical framework to analyze the performance of V-D2D communications underlaying cellular networks, by taking the unique characteristics of VANETs into consideration. To the best of our knowledge, our study is first of this kind to look into this emerging topic. Specifically, we model the urban road layout as a grid-like pattern. The cellular coverage areas are thus also considered as a square area, with the capability to extend to any other coverage patterns. The density of vehicles is modeled by non-homogeneous distributions in the considered area, because vehicles are more likely to move around social spots [15]. We then apply D2D communication in the modeled VANETs scenario. A channel inversion transmit power control mechanism is utilized to keep the receive power to be a threshold ρ_0. In addition, we employ a biased channel quality based mode selection strategy, where a biased factor φ explicitly controls the preference on V-D2D mode over cellular mode. Based on these models, two critical performance metrics, signal-to-interference-plus-noise (SINR) outage probability and link/network throughput, are theoretically analyzed, and the relation with the important design parameters ρ_0 and φ is obtained, followed by simulation validation. A counter-intuition observation is found that the network throughput does not always increase with larger φ (more D2D transmissions). Plus, the impact of φ on the network throughput also depends on ρ_0. The contributions of the paper are as follows:

- Our proposed V-D2D underlay cellular network is governed by simple yet effective mechanisms. In particular, a channel inversion power control scheme avoids high interference level in V-D2D system, and a biased mode selection strategy based on channel quality optimally controls the appropriate portion of vehicular users selecting D2D mode or cellular mode;
- Our proposed theoretical framework, which takes into account the unique characteristics of VANETs, is able to systematically evaluate the performance of V-D2D underlay cellular networks. We specifically examine the impact of inversion power control mechanism and biased mode selection strategy on such V-D2D networks. Two most critical performance metrics – SINR outage probability and throughput – are thoroughly analyzed and systematically validated via extensive simulations. The relation between performance metrics and design parameters offers deep insights on the emerging V-D2D communications underlaying cellular network.

The proposed analytical framework provides theoretical insights into the performance of emerging V-D2D underlaying cellular networks. For cellular network operators, our framework not only offers guidelines to plan and deploy such cellular infrastructures and better utilize cherished spectrum resource, but also obtains the close-form relation between critical performance metrics and major system design parameters that could be used to further optimize the system efficiency of V-D2D networks.

The remainder of the paper is organized as follows. Section II studies the related works. Section III describes the system model. Section IV theoretically analyzes the network performance, followed by framework validation via simulation in Section V. Finally, Section VI concludes the paper.

II. STATE OF THE ART

D2D underlaying communications in cellular network has been extensively investigated. By utilizing spatially proximate communication opportunities, the spectrum efficiency of cellular network can be greatly improved. However, the interference introduced by D2D communications should be carefully managed. Interference management techniques such as interference reduction [16]–[20] and interference avoidance [21]–[23] have been proposed and discussed to manage the interference and improve the spectrum efficiency.

As one important topic, the performance of D2D communications underlaying cellular networks has also been well studied in the literature. In [24], Ni *et al.* analyzed the throughput bound of underlaying D2D communications. To manage the interference, different guard distances are introduced, including the guard distance between a D2D receiver and D2D transmitters and transmitting cellular user equipments (CUEs), and the guard distance between D2D transmitters and cellular base station (BS). Based on the geometric model, the maximum number of concurrent D2D communications is analyzed, and the impact of different parameters is studied. In [22], Min *et al.* analyzed the capacity of a D2D underlaying network in which a D2D user and M cellular users share a uplink channel (multiple antennas are employed). To enhance the overall network capacity, a δ_D-interference limited area control scheme is proposed, in which CUEs are not allowed to transmit within the area where the transmission will cause interference to a D2D receiver higher than a predefined threshold. Then, the coverage of δ_D-interference limited area is analyzed and the lower bound of the ergodic capacity is derived as a closed form. Many works studied the performance of D2D communication through stochastic geometry analysis [14], [25], [26]. In [14], Elsawy *et al.* introduced the mode selection and power control models for D2D-enabled uplink cellular networks. D2D users, cellular uplink users, and cellular BSes are modeled by independent PPPs with different intensities, and a truncated power control model as well as a mode selection strategy are employed. The performance metrics, i.e., the average SINR outage probability and link spectrum efficiency, are theoretically analyzed. In [25], Lin *et al.* proposed a tractable hybrid network model in which the D2D user locations are modeled by a PPP, based on which a unified performance analysis approach is proposed, and the expressions of analytical rate are obtained for both overlay and underlay D2D transmission. In spite of the rich research works of D2D communications, the results of existing works cannot be directly applied to VANETs, where the vehicle locations cannot be modeled by a PPP.

There are also several works that investigate the issues of applying D2D communications in VANETs. In [8], Cheng *et al.* studied the feasibility of D2D communication for the

intelligent transportation systems (ITS), considering the spatial distribution of vehicles, and the channel characteristics given the high mobility of vehicles. Through a simulation study, it is observed that the D2D-underlay mode achieves the highest spectrum efficiency, and the data rate increases with the decrease of D2D distance. In addition, the average spectrum efficiency first increases, then decreases with the increase of V-D2D link density, due to that when V-D2D link density is high, the interference becomes severer. In [27], Sun *et al.* proposed a spectrum resource allocation scheme for both cellular user equipments (CUEs) and vehicular UEs, in order to maximize the CUEs' sum rate while guarantee the strict delay and reliability requirements of VUEs' services. In [28], Ren *et al.* proposed a joint channel selection and power control framework to achieve optimal performance of V-D2D system, where a series simplifications are made to reduce the requirement of full channel state information (CSI).

In a nutshell, although the D2D communication technology has been intensively discussed, the research of vehicular D2D communication is still in its beginning stage, with many open issues. On one hand, the high mobility of vehicles and variable traffic load can greatly affect the signal propagation, and makes it difficult to obtain reliable CSI which is required for accurate resource allocation in D2D communication. On the other hand, the correlation of vehicles (e.g., vehicle clusters) and the awareness of location information (e.g., GPS devices) can provide more opportunity to the location-based V-D2D applications. In this paper, we focus on V-D2D communications underlaying cellular network in urban area, apply power allocation and mode selection schemes, and theoretically analyze the network performance.

III. SYSTEM MODEL

In this section, the system model of the analytical framework is presented. We first describe the street pattern of the considered area, followed by the network model, including the D2D and cellular transmission distances, the transmit power control, and channel characteristics. Then, the mode selection strategy is given, where a bias factor φ is used to reflect the preference of D2D transmissions over cellular transmissions. A summary of the mathematical notations used in this paper is given in Table I.

A. Street Pattern

We consider an urban area fully covered by the LTE cellular network. The considered area has a grid-like street pattern, as the downtown area of many cities, such as Houston and Portland [29]. The network geometry consists of a set of north-south (vertical) roads intersected with a set of east-west (horizontal) roads, as shown in Fig. 1. The lengths of each road segment r_i are identical, which is denoted by L, leading to equal-sized square street blocks with side length L. We further consider the coverage area of an LTE eNB to be a square, with the side length M normalized by L. Also denote the considered cellular coverage area by Ω_C. Note that we consider M is even in the analysis, while the methodology can be easily applied when M is odd. Denote the set of

Table I
USEFUL NOTATIONS

| Symbol	Description
r_i	Road segment i
L	Length of a road segment
Ω_C	The considered cellular coverage area
Ω_T	Inter-cell interference area of Ω_C
M	Side length of Ω_C
ϵ_i	Vehicle density on r_i
d_D	D2D transmission distance
$d_{C,i}$	Cellular uplink distance of r_i
γ_C, γ_D	Path-loss exponent of cellular transmission and D2D transmission
h	Channel gain
ρ_0	Receive power threshold
φ	Bias factor
$Z_{C,i}, Z_{D,i}$	Transmit power given D2D (resp. cellular) mode is selected
$\mathcal{I}$	Interference
η	Signal-to-interference-plus-noise ratio (SINR)
$p_{o,i}(\omega)$	SINR outage probability, where ω is SINR outage threshold
n_0	Noise power
σ	Average link throughput
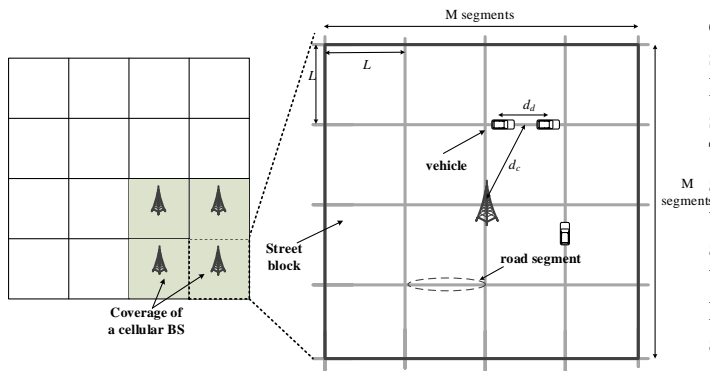
Figure 1. System model.

road segments within a cellular coverage area by $\mathcal{M}_\mathcal{C}$ with $|\mathcal{M}_\mathcal{C}| = 2M(M+1)$. There are two things worth to be noted. First, we focus on the urban area because in these areas V-D2D communication is more urgent due to the heavy-loaded data traffic, and we will leave the analysis of suburban and rural areas in the future works; second, the analysis can be easily applied to coverage patterns other than the square pattern, such as hexagon coverage, and Vorinoi coverage which is a common coverage pattern of LTE networks.

The density of vehicles in road segments can impact the network performance, since V-D2D communication can happen only when two vehicles are close to each other. According to [30], the vehicle density at a location can be accurately modeled by different heavy-tail distributions, such as Weibull, log-logistic, and log-gamma distribution. We consider that on road segment r_i, the probability density function (PDF) and cumulative density function (CDF) of the vehicle density ϵ_i are $f_{\epsilon,i}(x)$ and $F_{\epsilon,i}(x)$, respectively.

B. Network Model

The FDD LTE network is considered, where uplink and downlink transmissions use orthogonal sets of channels. We

consider V-D2D communications for vehicle-to-vehicle data services in this paper, e.g., direct video/audio streaming or Internet contents sharing, while vehicle-to-infrastructure data services can be supported by normal cellular transmissions. Two VUEs can transmit data via the cellular network, and as an alternative, if close to each other, they can transmit directly without going through the LTE, i.e., V-D2D transmissions. It is assumed that V-D2D transmissions can happen only when two VUEs are in the same road segment r_i, for the reasons that V-D2D transmissions are only available for vehicles in proximity, and it is usually difficult for the signal to transmit between two intersected road segments in urban areas due to the block of buildings. In addition, vehicles in the same road segment are more likely to preserve a longer and more reliable connection, which avoids frequent D2D connection set up and tear down. Therefore, the eNB can schedule V-D2D communication only within one road segment. A similar consideration can be found in [15]. Since the existence of a transmission in r_i requires no less than two vehicles in r_i, the probability a transmission request exists in r_i can then be calculated by $p_{T,i} = 1 - F_{\epsilon,i}(2)$. Then, the D2D transmission distance $d_D \in [0, L]$ [1]. It is further considered that within a road segment r_i, the location of an arbitrary VUE follows a uniform distribution, which means that within r_i, a VUE appears in any location equally likely. Consequently, given that a V-D2D link exists in r_i, the V-D2D transmission distance $d_{D,i}$ follows a triangular distribution, and thus the PDF of $d_{D,i}$ can be expressed by

$$f_{d_{D,i}}(x) = \frac{2}{L}(1 - \frac{x}{L}). \qquad (1)$$

Since $f_{d_{D,i}}(x)$ does not depend on i, D2D transmission distances in all road segments are independent and identically distributed (*i.i.d.*) random variables with the PDF given in (1). Note that the distribution of locations a vehicle may appear in a road segment can be extended to a general model, and

---

[1] Since the D2D communication often involves bi-directional communication, we do not differentiate D2D transmitter and receiver in this paper.

the distribution of V-D2D distances can be obtained in a similar way. For cellular uplink transmission, denote by $d_{C,i}$ the cellular uplink distance if the transmitting VUE is in r_i. For the simplicity of analysis, we consider that $d_{C,i}$ is independent of $d_{D,i}$, and is approximated by the distance from the eNB to the middle point of r_i, due to that usually the cellular uplink distance is much larger than the D2D distance. Therefore, due to the symmetry of the road pattern, the probability mass function (PMF) of the cellular uplink distance $d_{C,i}$, denoted by $p_{d_C}(x)$, can be easily obtained as

$$p_{d_C}(x) = \begin{cases} \frac{4}{|\mathcal{M}_C|}, & x = \frac{L}{2} \\ \frac{8}{|\mathcal{M}_C|}, & x = \frac{\sqrt{5}L}{2} \\ \frac{4}{|\mathcal{M}_C|}, & x = \frac{3L}{2} \\ \frac{8}{|\mathcal{M}_C|}, & x = \frac{13L}{2} \\ \cdots \end{cases} \quad (2)$$

Due to the high mobility of vehicles, the rapid channel variations results in difficulty in obtaining real-time full CSI which contains the actual channel fading parameters. Thus, large-scale fading effects including path loss and shadowing are preferred when designing V-D2D communication protocols [27], [28], [31]. In [8], a simulation has been conducted, showing that the performance degradation of V-D2D communication is very little when only path loss is considered. Based on these observations, in this paper, we only consider the large-scale fading effects. Following [14] and [19], we consider a general power-law path-loss model with the decay rate $d^{-\gamma}$, where d is the distance between the transmitter and the receiver, and $\gamma > 2$ is the path-loss exponent. The cellular uplink and V-D2D links may have different path-loss exponents, denoted by γ_C and γ_D, respectively. We consider a Rayleigh fading environment[2], where the channel gain h between any two locations follows *i.i.d.* exponential distribution with unit mean, i.e., $h \sim exp(1)$.

The transmit power is regulated by a channel inversion power control model, in which the path-loss is compensated by the transmit power such that the average received signal power at the intended receiver (i.e., eNB for uplink transmissions and receiving VUE for V-D2D transmission) equals a certain receive power threshold ρ_0. Therefore, the instant received power can be expressed by $\rho_0 h$. In general, if the channel inversion power control is employed, a power truncate outage may happen due to that the required transmit power is larger than the maximum transmit power P_m [14]. However, in the considered urban V-D2D scenario, power truncate outage does not happen since P_m is large enough to compensate the path-loss of a cellular edge transmission, the distance of which is much larger than the maximum D2D transmission distance L. The V-D2D communications underlaying cellular network may have multiple channels. However, since the interference statistics of all channels are similar, we restrict our analysis to one channel, which is shared by V-D2D transmissions and maximum one uplink transmission in the considered cellular coverage area.

[2]Methods to relax to general fading models can be found in [32]

C. Mode Selection Strategy

VUEs can transmit data using either cellular mode or D2D mode. In cellular mode, eNB routed two-hop transmission is employed: the data packet is first transmitted from the transmitting VUE to the eNB through uplink channels, and then from the eNB to the receiving VUE through downlink channels. In D2D mode, two VUEs can directly transmit data reusing the cellular uplink resources. The cellular uplink resources are reused by V-D2D transmissions, since the interference caused at the BS can be efficiently managed [33]. The mode selection greatly impacts the network performance. If more VUEs select D2D mode, the frequency spatial reuse can be improved; however, more interference is introduced to both D2D and cellular uplink transmissions. Therefore, more D2D transmissions do not always enhance the throughput or offloading performance, as demonstrated in [8].

In this paper, we employ a biased channel quality based mode selection strategy to model the tradeoff among SINR, frequency reuse, throughput, and offloading performance. In the biased channel quality based mode selection, a VUE selects D2D mode if the biased quality of D2D channel is no worse than the quality of the cellular uplink channel, i.e.,

$$\varphi d_D^{-\gamma_D} \geq d_C^{-\gamma_C}; \quad (3)$$

otherwise, the cellular mode will be chosen. The bias factor φ reflects the preference on D2D mode over cellular mode, where a larger φ indicates that D2D transmissions are more likely to happen, leading to higher frequency reuse and more interference. With this model, the interference to the cellular uplink transmissions can be controlled. To satisfy (3), a D2D transmission closer to the eNB tends to have a smaller transmission distance d_D, and a correspondingly smaller transmit power due to the channel inversion power control. We show that the interference power from any D2D transmission to the eNB can be upper bounded by $\varphi\rho_0$ in Appendix A. Fig. 2 shows the mode selection results in terms of φ, in a scenario with $L = 100$ m and $M = 10$. It can be seen that the number of V-D2D transmissions (shown as red dots) increases when the value of φ becomes larger, since a larger φ indicates D2D mode is more preferred. Moreover, in the area closer to the BS, the D2D transmission is less likely to happen, which protects the cellular uplink transmission from severe interference.

Under the mode selection strategy, we can calculate the probability that D2D/cellular mode is selected. In road segment r_i, the cellular uplink distance $d_{C,i}$ is a constant. Thus, given a transmission request among two VUEs in r_i, the probability that D2D mode is selected can be obtained by

$$\begin{aligned} p_{D,i} &= \mathbb{P}(\varphi d_{D,i}^{-\gamma_D} \geq d_{C,i}^{-\gamma_C}) \\ &= F_{d_D}(\varphi^{\frac{1}{\gamma_D}} d_{C,i}^{\frac{\gamma_C}{\gamma_D}}) \\ &= \frac{\varphi^{\frac{1}{\gamma_D}} d_{C,i}^{\frac{\gamma_C}{\gamma_D}}}{L}(2 - \frac{\varphi^{\frac{1}{\gamma_D}} d_{C,i}^{\frac{\gamma_C}{\gamma_D}}}{L}), \end{aligned} \quad (4)$$

where $F_{d_D}(\cdot)$ is the cumulative density function (CDF) of D2D distance d_D. Accordingly, the probability that the cellular mode is selected is $p_{C,i} = 1 - p_{D,i}$.
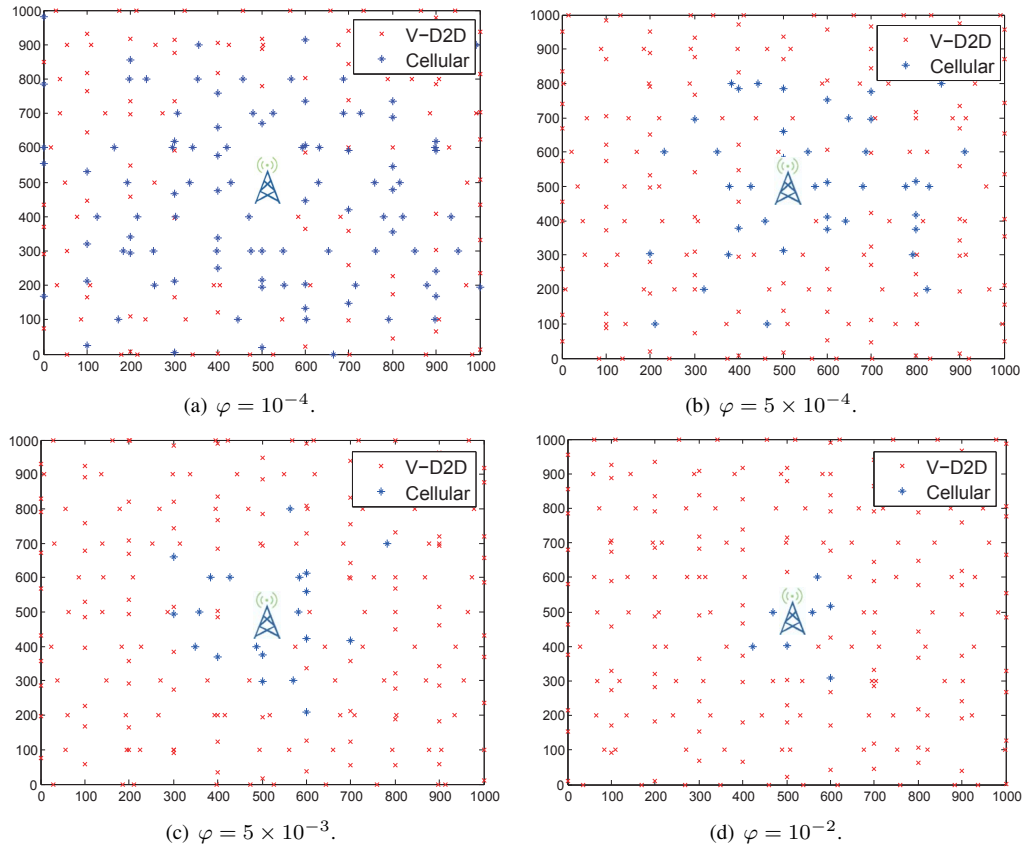
Figure 2. Mode selection result.

IV. NETWORK PERFORMANCE ANALYSIS

In this section, we analyze the performance of the V-D2D communications underlaying cellular networks. We start with the probability distribution of the transmit power of an arbitrary V-D2D transmission and cellular uplink transmission. Then, we analyze the interference from both V-D2D transmissions and uplink transmission in the considered cellular coverage area and the first tier around the considered cellular coverage area, based on which the probability distribution of SINR is derived. Then, the performance metrics, the SINR outage probability and throughput, are theoretically obtained. Note that for integer values of path loss exponents, the SINR outage probability can be expressed in closed-form.

A. Transmit power

In this part, we analyze the transmit power of both D2D mode and cellular mode. According to the channel inversion power control and mode selection model, the maximum D2D transmission power in road segment r_i is $P_{D_{m,i}} = \min(P'_{D_m}, \varphi \rho_0 d_{C,i}^{\gamma_C})$, where $P'_{D_m} = \rho_0 L^{\gamma_D}$ is the maximum transmit power due to the maximum V-D2D distance L, and $\varphi \rho_0 d_{C,i}^{\gamma_C}$ is the maximum transmit power due to the mode selection strategy. Given D2D mode is selected, the D2D transmit power $Z_{D,i}$ is the transmit power required to compensate the path-loss conditioned on $\varphi d_{D,i}^{-\gamma_D} \geq d_{C,i}^{-\gamma_C}$, i.e., $Z_{D,i} = \{P_{D,i} : \varphi d_{D,i}^{-\gamma_D} \geq d_{C,i}^{-\gamma_C}\}$, where $P_{D,i}$ is the unconditioned V-D2D transmit power. The PDF of $Z_{D,i}$ is given in Lemma 1.

Lemma 1: In the urban V-D2D communication underlaying cellular network with channel inversion power control and biased channel quality based mode selection, the PDF of the D2D transmit power in r_i, denoted by $Z_{D,i}$, is given by

$$f_{Z_{D,i}}(x) = \frac{1}{p_{D,i}} \left(\frac{2x^{\frac{1}{\gamma_D}-1}}{\gamma_D L \rho_0^{\frac{1}{\gamma_D}}} - \frac{2x^{\frac{2}{\gamma_D}-1}}{\gamma_D L^2 \rho_0^{\frac{2}{\gamma_D}}} \right), Z_{D,i} \leq P_{D_{m,i}},$$

(5)

where $P_{D_{m,i}} = \min(P'_{D_m}, \varphi \rho_0 d_{C,i}^{\gamma_C})$.

Proof: See Appendix B. ∎

For cellular mode, the transmit power $Z_{C,i}$ is the transmit power from the VUE to the eNB (denoted by $P_{C,i}$) conditioned on $\varphi d_{D,i}^{-\gamma_D} < d_{C,i}^{-\gamma_C}$. Since $P_{C,i} = \rho_0 d_{C_i}^{\gamma_C}$ is a constant, $Z_{C,i} = P_{C,i} = \rho_0 d_{C_i}^{\gamma_C}$ is a constant. The PMF of $Z_{C,i}$ and Z_C is described in the following lemma.

Lemma 2: In the urban V-D2D communications underlaying cellular network with channel inversion power control and biased channel quality based mode selection, the cellular uplink transmit power in r_i, denoted by $Z_{C,i}$, is a constant $Z_{C,i} = \rho_0 d_{C_i}^{\gamma_C}$.

Proof: The transmit power of a VUE is a constant equal to $\rho_0 d_C^{\gamma_C}$. Therefore, given the cellular mode is selected, the transmit power remains unchanged. ∎

B. Interference and signal-to-interference-plus-noise ratio

In cellular networks, the interference is caused by co-channel transmissions in the same cell and neighboring cells,
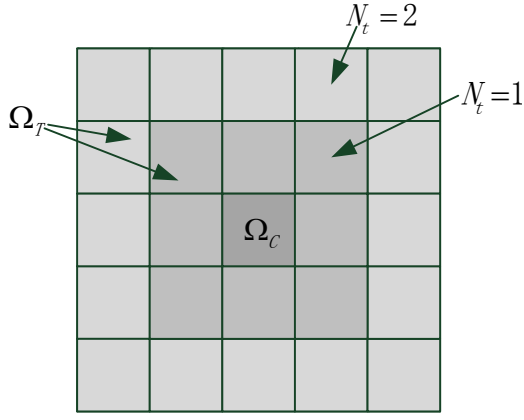
Figure 3. Interference area with $N_t = 2$.

which is called intra-cell interference and inter-cell interference, respectively. In V-D2D communications underlaying cellular networks, the interference is caused by not only cellular uplink transmission, but also D2D transmissions which reuse uplink resources. In this part, we consider intra-cell and inter-cell interference from both cellular uplink transmissions and V-D2D transmissions. For inter-cell interference, we consider the interference from N_t tiers of cells around the considered cell, as shown in Fig. 3. Usually considering $N_t = 1$ is sufficient to analyze the inter-cell interference, and the interference power from transmissions of even further areas can be considered as noise.

Denote the considered cellular coverage area by Ω_C, the area where inter-cell interference originates by Ω_T, and $\Omega_I = \Omega_C + \Omega_T$. Denote the sets of road segments in Ω_C, Ω_T, and Ω_I by $\mathcal{M}_\mathcal{C}$, $\mathcal{M}_\mathcal{T}$, and $\mathcal{M}_\mathcal{I}$, respectively. Consider a D2D/uplink transmission in road segment $r_i \in \mathcal{M}_\mathcal{C}$. The total interference to the D2D/uplink transmission can be expressed by

$$\mathcal{I}_i = \mathcal{I}_{\mathcal{D},i} + \mathcal{I}_{\mathcal{C},i}$$
$$= \sum_{r_j \in \mathcal{M}_\mathcal{I} \backslash r_i} \mathbb{1}_{D,j} Z_{D,j} h d_{ji}^{-\gamma_D} + \mathbb{1}_{C,j} Z_{C,j} h d_{ji}^{-\gamma_C}, \quad (6)$$

where $Z_{D,i}$ (resp. $Z_{C,i}$) is the transmit power of V-D2D (resp. cellular uplink) transmission in road segment r_i. d_{ji} is the distance from the interferer to the receiver, and d_{j0} denotes the distance from the interferer to the eNB of Ω_C. For simplicity, when the interference to the V-D2D transmission is considered, d_{ji} is the distance between the middle points of r_j and r_i; when the interference to uplink transmission is considered, d_{j0} is the distance from the middle point of r_j to the location of eNB of Ω_C. $\mathbb{1}_{D,i}$ and $\mathbb{1}_{C,i}$ are indicator functions where $\mathbb{1}_{X,i} = 1$ if a transmission request exists in r_i and chooses mode X, and $\mathbb{1}_{X,i} = 0$ otherwise. Based on the vehicle density distribution and the mode selection strategy, $\mathbb{P}(\mathbb{1}_{D,i} = 1) = p_{T,i} p_{D,i}$. Furthermore, for the analysis tractability, we consider that cellular uplink scheduling is round-robin [14]. Therefore, when $|\mathcal{M}_\mathcal{C}|$ becomes larger, the probability that no transmission selects cellular mode gets smaller (i.e., $\prod_{r_i \in \mathcal{M}_\mathcal{C}} 1 - p_{T,i}(1 - p_{D,i})$ gets smaller), and $\mathbb{P}(\mathbb{1}_{C,i} = 1) \approx \frac{p_{T,i}(1-p_{D,i})}{\sum_{r_i \in \mathcal{M}_\mathcal{C}} p_{T,i}(1-p_{D,i})}$.

With the total interference $\mathcal{I}_i$ given in (6), the signal-to-interference-plus-noise ratio (SINR) of a D2D/uplink transmission in road segment $r_i \in \mathcal{M}_\mathcal{C}$ can be expressed by

$$\eta_i = \frac{\rho_0 h}{n_0 + \sum_{r_j \in \mathcal{M}_\mathcal{I} \backslash r_i} \mathbb{1}_{D,j} Z_{D,j} h d_{ji}^{-\gamma_D} + \mathbb{1}_{C,j} Z_{C,j} h d_{j0}^{-\gamma_C}}, \quad (7)$$

where n_0 is the noise power.

C. Performance metrics

V-D2D communications can improve the frequency spatial reuse, and therefore the spectrum efficiency and throughput can be increased. On the other hand, more interference is introduced, resulting in decreasing SINR for both D2D and cellular transmissions. Therefore, in this part, we consider two performance metrics, i.e., SINR outage probability and throughput, to analyze the performance of the V-D2D communications underlaying cellular network.

Given the SINR outage threshold ω, the SINR outage probability of the transmission in r_i is

$$p_{o,i}(\omega) = \mathbb{P}(\eta_i \leq \omega)$$
$$= \mathbb{P}(h \leq \frac{\omega}{\rho_0}(n_0 + \mathcal{I}_{\mathcal{D},i} + \mathcal{I}_{\mathcal{C},i}))$$
$$\overset{i}{=} 1 - \exp\{-\frac{\omega}{\rho_0}(n_0 + \mathcal{I}_{\mathcal{D},i} + \mathcal{I}_{\mathcal{C},i})\}$$
$$\overset{ii}{=} 1 - \exp\{-\frac{\omega n_0}{\rho_0}\} \mathcal{L}_{\mathcal{D},i}(\frac{\omega}{\rho_0}) \mathcal{L}_{\mathcal{C},i}(\frac{\omega}{\rho_0}), \quad (9)$$

where $\mathcal{L}_\mathcal{X}(\cdot)$ denotes the Laplace transform of the PDF of the random variable, when mode X is chosen, and $\mathcal{L}_{\mathcal{D},i}(\cdot)$ and $\mathcal{L}_{\mathcal{C},i}(\cdot)$ are calculated in Appendix C. In (9), (i) follows since h is a exponential random variable with unit mean, and (ii) follows because the transmission modes in each road segment are independent. Then, a V-D2D transmission in r_i, the SINR outage probability $p_{oD,i}(\omega)$ is given in (8), where $\mathcal{H}(\cdot)$ is hypergeometric function, and $\beta = -\frac{\omega}{\rho_0} d_{ji}^{-\gamma_D} P_{D_{m,i}}$. Therefore, the average V-D2D SINR outage probability in Ω_C, denoted by $p_{oD}(\omega)$, can be calculated by

$$p_{oD}(\omega) = \frac{\sum_{r_i \in \mathcal{M}_\mathcal{C}} p_{T,i} p_{D,i} p_{oD,i}(\omega)}{\sum_{r_i \in \mathcal{M}_\mathcal{C}} p_{T,i} p_{D,i}}. \quad (10)$$

For cellular uplink transmissions, the interference is caused at the eNB of Ω_C. Therefore, for an arbitrary cellular uplink transmission, the SINR outage probability can also be calculated by (8), where d_{ji} is replaced by d_{j0}. Note that for integer value of γ_C and γ_D, (8) has closed-form expression.

Another important performance metric is the link/network throughput. Since the V-D2D communications introduce interference to the network, the throughput of the cellular uplink is degraded. However, in the network level, the throughput can be enhanced by spatial spectrum reuse due to concurrent transmissions. The average link throughput in a unit spectrum (or spectrum efficiency) when the transmitter is in r_i, denoted

$$p_{oD,i}(\omega) = 1 - \exp(\frac{-\omega n_0}{\rho_0}) \prod_{r_j \in \mathcal{M}_\mathcal{I} \backslash r_i} \left(\frac{2p_{T,j} P_{D_{m,j}}^{\frac{1}{\gamma_D}} \mathcal{H}([1,\frac{1}{\gamma_D}],[1+\frac{1}{\gamma_D}],\beta)}{L\rho_0^{\frac{1}{\gamma_D}}} - \frac{p_{T,j} P_{D_{m,j}}^{\frac{2}{\gamma_D}} \mathcal{H}([1,\frac{2}{\gamma_D}],[1+\frac{2}{\gamma_D}],\beta)}{L^2 \rho_0^{\frac{2}{\gamma_D}}} + 1 - p_{D,j}p_{T,j} \right)$$
$$\cdot \frac{1}{\sum_{r_i \in \mathcal{M_C}} p_{T,i}(1-p_{D,i})} \sum_{r_j \in \mathcal{M}_\mathcal{I} \backslash r_i} \frac{p_{T,j}(1-p_{D,j})}{(1+sZ_{C,j}d_{ji}^{-\gamma_C})} \qquad (8)$$

by σ_i, can be calculated based on the SINR outage probability:

$$\sigma_i = \mathbb{E}[\log_2(1 + SINR_i)]$$
$$= \int_0^\infty \mathbb{P}(\log_2(1+SINR_i) > x)dx$$
$$= \int_0^\infty \mathbb{P}(\eta_i > 2^x - 1)dx$$
$$= \int_0^\infty 1 - p_{o,i}(2^x - 1)dx, \qquad (11)$$

where $p_{o,i}(\cdot)$ is the SINR outage probability given in (9). Therefore, the average total spectrum efficiency in a cellular coverage Ω_C can be calculated by

$$\sigma = \sum_{r_i \in \mathcal{M_C}} p_{T,i}\left(p_{D,i}\sigma_{D,i} + \frac{1-p_{D,i}}{\sum_{r_i \in \mathcal{M_C}} p_{T,i}(1-p_{D,i})}\sigma_{C,i}\right) \qquad (12)$$

D. Extension of the results

As mentioned in Section III, the analytical results obtained above are not limited to the grid-like street pattern and square cellular coverage area. In this part, we show how the results are extended to other scenarios where the street patterns are irregular, and the cellular coverage is more general, such as hexagon and Vorinoi coverage, provided that the geographic information and vehicle density of each road segment is known.

Consider an urban area with a set of road segment $\mathbf{r} = \{r_1, r_2, \ldots, r_W\}$. For each road segment r_i, the geographic information such as the locations of end points is known. This information can be obtained from geo-location databases such as TIGER/Line Shapefiles [34]. The vehicle density in r_i is denoted by ϵ_i, with the PDF and CDF denoted by $f_{\epsilon,i}(x)$ and $F_{\epsilon,i}(x)$, respectively. Consider a cellular coverage area Ω_C, the set of road segment $\mathbf{r}$ is divided into two subsets, $\mathbf{r_c}$ the set of road segments within Ω_C, and $\bar{\mathbf{r_c}}$ the set of road segments outside Ω_C. Then, we can calculate the SINR of uplink/D2D transmissions in road segment $r_i \in \mathbf{r_c}$ by a method similar to (7):

$$\eta_i = \frac{\rho_0 h}{n_0 + \sum_{r_j \in \mathbf{r} \backslash r_i} \mathbb{1}_{D,j}Z_{D,j}hd_{ji}^{-\gamma_D} + \mathbb{1}_{C,j}Z_{C,j}hd_{j0}^{-\gamma_C}}, \qquad (13)$$

where d_{ji} and d_{j0} can be calculated from the geographic information of road segments. With SINR obtained, the performance metrics such as SINR outage probability and spectrum efficiency can be then theoretically analyzed similar to the methods in Section IV-C.

V. EVALUATION

In this section, we conduct a simulation to validate the proposed analytical framework. In an urban area with grid-like road system, the length of road segment $L = 100$ m, and the side length of a cellular BS coverage area is set to $M = 10$ road segments. Each road segment has two lanes with bidirectional vehicle traffic. We use VANETMobisim [35] to generate the mobilities of vehicles. Speed limit is set to 50 km/h. The vehicle mobility is controlled by Intelligent Driver Model with Lane Changes (IDMLC) model, in which vehicle speed is based on movements of vehicles in neighborhood. Unless otherwise stated, we set the channel inversion threshold $\rho_0 = -80$ dBm, noise power $N_0 = -90$ dBm, the path-loss exponents $\gamma_C = \gamma_D = 4$ [36], the SINR outage threshold $\omega = 2$, and $N_t = 1$ tier of cells where inter-cell interference is considered. All simulation results are plotted with 90% confidence intervals.

In the simulation, two arbitrary vehicles in the same road segment can request a transmission between each other. If more than two transmission requests happen in the same road segment, the cellular network randomly schedules one request with V-D2D transmission (called potential V-D2D transmission), and schedules the others to use traditional cellular transmissions, i.e., the transmitter-BS-receiver two-hop transmissions. A potential V-D2D transmission selects the D2D mode if the D2D selection condition (3) is satisfied; otherwise, the cellular mode is selected. Note that only one cellular uplink transmission can be scheduled in one time and sub-channel.

Fig. 4 shows the average SINR outage probability in the considered area Ω_C, including V-D2D transmissions and cellular uplink transmissions, with respect to (w.r.t.) the SINR outage threshold ω, and varied values of ρ_0 and φ. Straightforwardly, the SINR outage probability increases with the increase of the outage threshold ω. Different vehicular services and applications may require different data rates, which correspond to different SINR requirements. Thus, the results of Fig. 4 indicate that for data-craving applications, such as high-quality video streaming, the SINR outage probability could be higher, which can be an important design concern of the V-D2D communications underlaying cellular network. Fig. 4(a) shows the impact of the channel inversion threshold ρ_0 on the SINR outage probability. ρ_0 influence the SINR in two different ways. On one hand, with a smaller value of ρ_0, the V-D2D/cellular transmitters can use a smaller power, and thus cause less interference to each other; on the other hand, the received signal power $\rho_0 h$ is also smaller. In the simulated scenario, the latter, i.e., the impact on the received signal power dominates, and thus the SINR outage probability
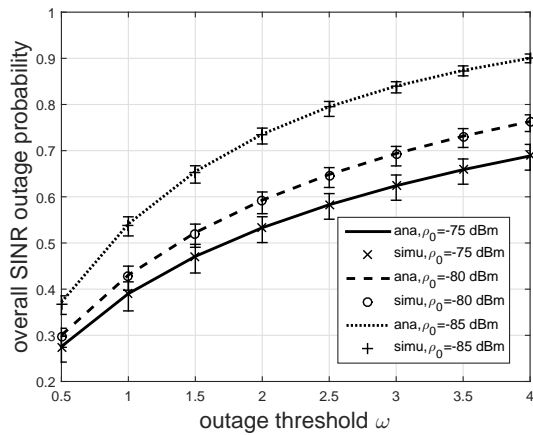
(a) Varied channel inversion threshold ρ_0.
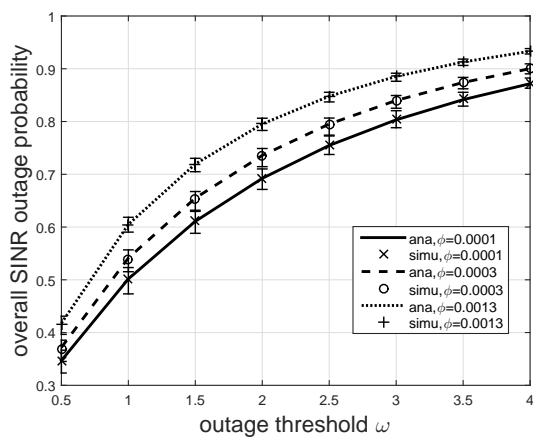
(b) Varied bias factor φ.

Figure 4.   SINR outage probability w.r.t. ω.

Figure 5.   SINR outage probability w.r.t. φ.

increases with the decrease of ρ_0. Note that the conclusion may vary with different VANETs topology patterns and topology parameters L and M, the analysis of which is considered one of our future works. Fig. 4(b) shows the impact of the bias factor φ on the SINR outage probability. With a larger value of φ, more transmission requests will choose D2D mode, which in turn causes more interference, and results in higher SINR outage probability.

Fig. 5 shows the SINR outage probability w.r.t. the bias factor φ. One important observation is that the SINR outage probability increases monotonously with φ. Different from ρ_0, φ does not impacts the received signal power, but influence the interference in the following ways. First, a higher value of φ leads to a higher D2D selecting probability according to (4), and thus more concurrent transmissions. Second, with a higher value of φ, it is more likely for V-D2D transmission to use a higher transmit power based on (5). Therefore, a higher value of φ will lead to a higher level of interference, and thus result in a higher average SINR outage probability. However, a higher average SINR outage probability does not necessarily indicate a lower cell throughput, which will be discussed later. When φ surpasses a certain value, most of V-D2D transmissions can use the possibly maximum transmit power,
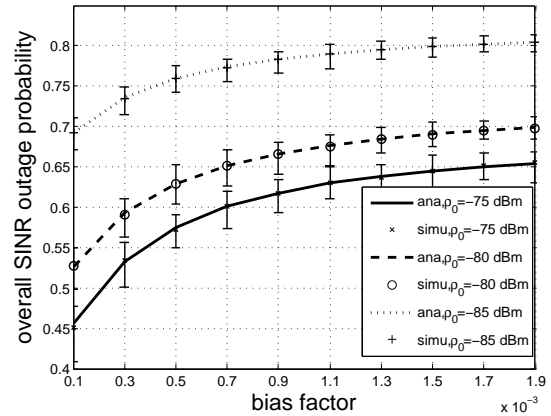
i.e., $P_{D_m,i} = \min\left(P'_{D_m}, \varphi\rho_0 d_{C,i}^{\gamma_C}\right) = P'_{D_m}$, and consequently further increasing φ will have little impact on the SINR outage probability, as shown in Fig. 5 where $\varphi > 0.9 \times 10^{-3}$.

Fig. 6 shows the throughput performance of the V-D2D underlaying cellular network w.r.t. the bias factor φ. The throughput is presented in the form of spectrum efficiency, and thus the unit is bits/s/Hz. It can be seen that a larger value of channel inversion threshold ρ_0 leads to a higher throughput due to a higher SINR, as discussed in Fig. 4(a). In Fig. 6(a), we consider the average throughput of the cellular uplink transmission, i.e., $\sigma_C = \sum_{r_i \in \mathcal{M}_C} \frac{p_{T,i}(1-p_{D,i})}{\sum_{r_i \in \mathcal{M}_C} p_{T,i}(1-p_{D,i})}\sigma_{C,i}$, which reflects the cellular uplink throughput from the perspective of the network operator. As shown in the figure, the cellular uplink throughput decreases with the increase of φ. This is because with a larger φ, both D2D selecting probability and D2D transmission power increase, resulting in a larger interference at the BS. The SINR of the cellular uplink transmissions thus decreases, leading to a lower throughput. Different from Fig. 5, even when φ is large, there is still an obvious decrease of the cellular uplink throughput with the increase of φ. This is because the throughput of cellular uplink is mainly influenced by the D2D transmissions in the road segments close to the BS. When φ is large, the transmit power of these transmissions still increases with φ, as $P_{D_m,i} = \min\left(P'_{D_m}, \varphi\rho_0 d_{C,i}^{\gamma_C}\right) = \varphi\rho_0 d_{C,i}^{\gamma_C}$, which causes more interference at the BS. Fig. 6(b) shows the total average throughput in a cellular coverage area, including all V-D2D transmissions and the cellular uplink transmission. By comparing to Fig. 6(a), it is shown that V-D2D communications can greatly boost the spectral efficiency of the cellular networks. Also, for different values of channel inversion threshold ρ_0, the bias factor φ impacts the throughput in different ways. For the cases of $\rho_0 = -75$ dBm and $\rho_0 = -80$ dBm, the total throughput increases from $\varphi = 0.1 \times 10^{-3}$ to 0.3×10^{-3}, but decreases slightly with the further increase of φ. This is because when φ is small, the interference is low, and with the increase of φ, there are more concurrent V-D2D transmissions, leading to larger total throughput. However, when φ is relatively large, the interference becomes the dominating factor, and thus the increase of φ leads to a decrease of total throughput. For
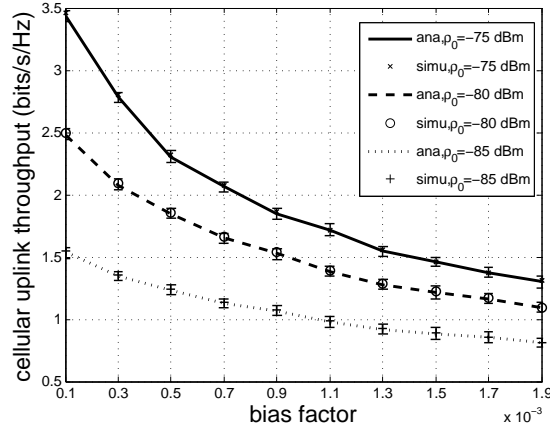
(a) Cellular uplink throughput.
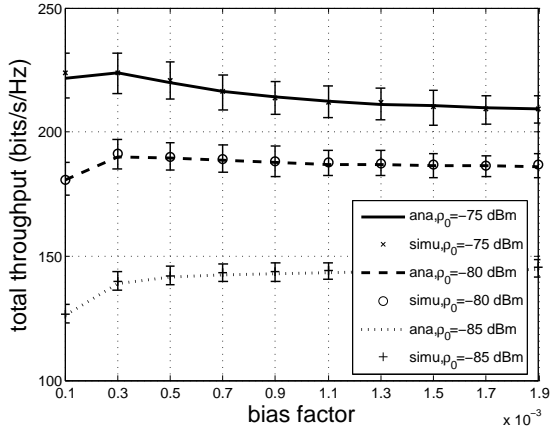
(b) Total throughput.

Figure 6.   Throughput performance w.r.t. φ.

the case of $\rho_0 = -85$ dBm, the total throughput increases with φ even when φ is larger than 0.3×10^{-3}. The reason is that when ρ_0 is small, the transmit power is small according to the channel inversion model, and thus the interference is small. Therefore, as the value of φ increases, more concurrent transmissions lead to a higher throughput. Compared with the results of Fig. 5, it can be seen that though the increase of φ degrades the SINR outage performance, it can influence the total throughput in varied ways.

VI. CONCLUSION

We have theoretically studied the performance of V-D2D underlaying cellular networks. We have modeled the urban road system, and the vehicle density distribution, and employed channel inversion model and biased channel quality based mode selection to control the transmit power and mode selection of vehicular users. Two performance metrics, SINR outage probability and throughput, have been theoretically analyzed. Simulation has been conducted, which validates our analysis, and shows the impact of design parameters on the performance metric. For future works, we will analyze the V-D2D performance in different scenarios, e.g., highway and more general road systems with varied intersection degrees (i.e., the number of roads connected to a intersection), lengths

of road segments, and sizes of the cellular coverage areas. In addition, considering the cost issues and user preferences, the network performance under different mode selection schemes, such as auction-based mode selection, will be studied.

APPENDIX

A. Upper bound of interference

Consider an arbitrary D2D transmission in road segment r_i. According to the mode selection, D2D mode is selected if $\varphi d_{D,i}^{-\gamma_D} \geq d_{C,i}^{-\gamma_C}$. Then, we have $d_{D,i}^{\gamma_D} \leq \varphi d_{C,i}^{\gamma_C}$, and the D2D transmit power $\mathbb{P}_{D,i} = \rho_0 d_{D,i}^{\gamma_D} \leq \varphi \rho_0 d_{C,i}^{\gamma_C}$. Therefore, the interference at the eNB from the D2D transmission is given by

$$I_{D,i}^C = \mathbb{P}_{D,i} d_{C,i}^{-\gamma_C} \leq \varphi \rho_0. \tag{15}$$

From (15), we can see that the interference from any D2D transmission to the cellular uplink transmission is upper bounded by $\varphi \rho_0$.

B. Lemma 1

Given D2D mode is selected, the D2D transmit power $Z_{D,i}$ is $Z_{D,i} = \{P_{D,i} : \varphi d_{D,i}^{-\gamma_D} \geq d_{C,i}^{-\gamma_C}\} = \{P_{D,i} : \rho_0 d_{D,i}^{\gamma_D} \leq \varphi \rho_0 d_{C,i}^{\gamma_C}\} = \{P_{D,i} : P_{D,i} \leq \varphi P_{C,i}\}$. Therefore, the PDF of $Z_{D,i}$ can be obtained by

$$
\begin{aligned}
f_{Z_{D,i}}(x) &= f_{P_{D,i}|P_{D,i} \leq \varphi P_{C,i}}(x) \\
&= \frac{f_{P_{D,i}}(x)}{\mathbb{P}(P_{D,i} \leq \varphi P_{C,i})} \\
&= \frac{1}{p_{D,i}} \left(\frac{2x^{\frac{1}{\gamma_D}-1}}{\gamma_D L \rho_0^{\frac{1}{\gamma_D}}} - \frac{2x^{\frac{2}{\gamma_D}-1}}{\gamma_D L^2 \rho_0^{\frac{2}{\gamma_D}}} \right),
\end{aligned}
\tag{16}
$$

where $P_{D,i}$ is obtained in (4), and $f_{P_{D,i}}(x)$ can be derived from the PDF of D2D distance d_D in (1) and the fact that $P_{D,i} = \rho_0 d_{D,i}^{\gamma_D}$.

C. Laplace transforms of $\mathcal{I}_C$ and $\mathcal{I}_D$

First we consider the interference from all V-D2D transmissions to a V-D2D transmission in road segment r_i, denoted by $\mathcal{I}_{\mathcal{DD},i}$. The Laplace transform of the PDF of $\mathcal{I}_{\mathcal{DD},i}$, denoted

$$\mathcal{L}_{\mathcal{I}_{\mathcal{DD},i}}(s) \overset{\gamma=4}{=} \prod_{r_j \in \mathcal{M}_\mathcal{I} \backslash r_i} p_{T,j} \Big\{ -\frac{d_{ji}^2 \arctan(\frac{\sqrt{sx}}{d_{ji}^2})}{L^2 \sqrt{\rho_0 s}} \Big\} + \frac{\sqrt{2}}{4} \frac{\frac{d_{ji}}{s^{\frac{1}{4}}} \ln\big(\frac{\sqrt{x} + \sqrt{2} x^{\frac{1}{4}} \frac{d_{ji}}{s^{\frac{1}{4}}} + \frac{d_{ji}^2}{\sqrt{s}}}{\sqrt{x} - \sqrt{2} x^{\frac{1}{4}} \frac{d_{ji}}{s^{\frac{1}{4}}} + \frac{d_{ji}^2}{\sqrt{s}}} \big)}{L \rho_0^{\frac{1}{4}}}$$

$$+ \frac{\sqrt{2}}{2} \frac{\frac{d_{ji}}{s^{\frac{1}{4}}} \arctan \frac{\sqrt{2} x^{\frac{1}{4}}}{d_{ji}} + 1}{L \rho_0^{\frac{1}{4}}} + \frac{\sqrt{2}}{2} \frac{\frac{d_{ji}}{s^{\frac{1}{4}}} \arctan \frac{\sqrt{2} x^{\frac{1}{4}}}{d_{ji}} - 1}{L \rho_0^{\frac{1}{4}}} + 1 - p_{D,j} p_{T,j} \qquad (14)$$

by $\mathcal{L}_{\mathcal{I}_{\mathcal{DD},i}}(s)$ can be calculated by

$$\mathcal{L}_{\mathcal{I}_{\mathcal{DD},i}}(s)$$
$$= \mathbb{E}[e^{-s \sum_{r_j \in \mathcal{M}_\mathcal{I} \backslash r_i} \mathbb{1}_{D,j} Z_{D,j} h d_{ji}^{-\gamma_D}}]$$
$$= \mathbb{E}[\prod_{r_j \in \mathcal{M}_\mathcal{I} \backslash r_i} e^{-s \mathbb{1}_{D,j} Z_{D,j} h d_{ji}^{-\gamma_D}}]$$
$$= \prod_{r_j \in \mathcal{M}_\mathcal{I} \backslash r_i} \mathbb{E}[e^{-s \mathbb{1}_{D,j} Z_{D,j} h d_{ji}^{-\gamma_D}}]$$
$$= \prod_{r_j \in \mathcal{M}_\mathcal{I} \backslash r_i} p_{D,j} p_{T,j} \mathbb{E}[e^{-s Z_{D,j} h d_{ji}^{-\gamma_D}}] + 1 - p_{D,j} p_{T,j}$$
$$= \prod_{r_j \in \mathcal{M}_\mathcal{I} \backslash r_i} \frac{2 p_{T,j} P_{D_{m,j}}^{\frac{1}{\gamma_D}} \mathcal{H}([1, \frac{1}{\gamma_D}], [1 + \frac{1}{\gamma_D}], \beta)}{L \rho_0^{\frac{1}{\gamma_D}}}$$
$$- \frac{p_{T,j} P_{D_{m,j}}^{\frac{2}{\gamma_D}} \mathcal{H}([1, \frac{2}{\gamma_D}], [1 + \frac{2}{\gamma_D}], \beta)}{L^2 \rho_0^{\frac{2}{\gamma_D}}} + 1 - p_{D,j} p_{T,j} \quad (17)$$

where $\mathcal{H}([\cdot], [\cdot], v)$ is hypergeometric function, and $\beta = -s d_{ji}^{-\gamma_D} \mathbb{P}_{D_{m,j}}$. Note that for integer values of γ_C and γ_D, (17) has closed-form expression. For example, when $\gamma_C = \gamma_D = 4$, $\mathcal{L}_{\mathcal{I}_{\mathcal{DD},i}}(s)$ is shown in (14), where $x = \mathbb{P}_{D_{m,j}}$.

The interference from all cellular uplink transmissions in Ω_I to a V-D2D transmission in road segment r_i is denoted by $\mathcal{I}_{\mathcal{CD},i}$. Similarly, the Laplace transform of the PDF of $\mathcal{I}_{\mathcal{CD},i}$, denoted by $\mathcal{L}_{\mathcal{I}_{\mathcal{CD},i}}(s)$ can be calculated by

$$\mathcal{L}_{\mathcal{I}_{\mathcal{CD},i}}(s)$$
$$= \mathbb{E}[e^{-s \sum_{r_j \in \mathcal{M}_\mathcal{I} \backslash r_i} \mathbb{1}_{C,j} Z_{C,j} h d_{ji}^{-\gamma_C}}]$$
$$= \mathbb{E}[\prod_{r_j \in \mathcal{M}_\mathcal{I} \backslash r_i} e^{-s \mathbb{1}_{C,j} Z_{C,j} h d_{ji}^{-\gamma_C}}]$$
$$= \sum_{r_j \in \mathcal{M}_\mathcal{I}} \mathbb{P}(\mathbb{1}_{C,j} = 1) \mathbb{E}[e^{-s Z_{C,j} h d_{ji}^{-\gamma_C}}]$$
$$= \frac{1}{\sum_{r_i \in \mathcal{M}_\mathcal{C}} p_{T,i} (1 - p_{D,i})} \sum_{r_j \in \mathcal{M}_\mathcal{I} \backslash r_i} \frac{p_{T,j}(1 - p_{D,j})}{(1 + s Z_{C,j} d_{ji}^{-\gamma_C})}.$$
$$\qquad (18)$$

When considering the interference to a cellular uplink transmission in road segment r_i, the calculation of $\mathcal{I}_{\mathcal{DC},i}$ and $\mathcal{I}_{\mathcal{CC},i}$ is similar to (17) and (18), by replacing d_{ji} with the distances from the road segments in $\mathcal{M}_\mathcal{I}$ to the BS of Ω_C.

REFERENCES

[1] N. Lu, N. Zhang, N. Cheng, X. Shen, J. W. Mark, and F. Bai, "Vehicles Meet Infrastructure: Towards Capacity-Cost Tradeoffs for Vehicular Access Networks," *IEEE Trans. on Intelligent Transportation Systems*, vol. 14, no. 3, pp. 1266–1277, 2013.

[2] H. A. Omar, N. Lu, and W. Zhuang, "Wireless access technologies for vehicular network safety applications," *IEEE Network*, to appear.

[3] K. Lee, J. Lee, Y. Yi, I. Rhee, and S. Chong, "Mobile data offloading: how much can WiFi deliver?" *IEEE/ACM Trans. on Networking*, vol. 21, no. 2, pp. 536–550, 2013.

[4] Cisco, "Cisco visual networking index: global mobile data traffic forecast update, 2014-2019." [Online]. Available: http://www.cisco.com/c/en/us/solutions/collateral/service-provider/visual-networking-index-vni/white_paper_c11-520862.pdf

[5] J. Ott and D. Kutscher, "Drive-thru Internet: IEEE 802.11b for automobile," in *Proc. of IEEE INFOCOM*, China, 2004.

[6] N. Cheng, N. Zhang, N. Lu, X. Shen, J. Mark, and F. Liu, "Opportunistic Spectrum Access for CR-VANETs: A Game-Theoretic Approach," *IEEE Trans. on Vehicular Technology*, vol. 63, no. 1, pp. 237–251, 2014.

[7] R. Lu, X. Lin, T. Luan, X. Liang, and X. Shen, "Pseudonym changing at social spots: An effective strategy for location privacy in VANETs," *IEEE Trans. on Vehicular Technology*, vol. 61, no. 1, pp. 86–96, 2012.

[8] X. Cheng, L. Yang, and X. Shen, "D2D for intelligent transportation systems: A feasibility study," *IEEE Trans. on Intelligent Transportation Systems*, to appear.

[9] A. Asadi, Q. Wang, and V. Mancuso, "A survey on device-to-device communication in cellular networks," *IEEE Communications Surveys & Tutorials*, vol. 16, no. 4, pp. 1801–1819, 2014.

[10] J. Liu, N. Kato, J. Ma, and N. Kadowaki, "Device-to-device communication in lte-advanced networks: a survey," *IEEE Communications Surveys & Tutorials*, vol. 17, no. 4, pp. 1923–1940, 2014.

[11] J. Liu, Y. Kawamoto, H. Nishiyama, N. Kato, and N. Kadowaki, "Device-to-device communications achieve efficient load balancing in lte-advanced networks," *IEEE Wireless Communications*, vol. 21, no. 2, pp. 57–65, 2014.

[12] L. Lei, Z. Zhong, C. Lin, and X. Shen, "Operator controlled device-to-device communications in LTE-advanced networks," *IEEE Wireless Communications*, vol. 19, no. 3, pp. 96–104, 2012.

[13] T. H. Luan, X. Shen, F. Bai, and L. Sun, "Feel bored? join verse! engineering vehicular proximity social networks," *IEEE Trans. on Vehicular Technology*, vol. 64, no. 3, pp. 1120–1131, 2015.

[14] H. ElSawy, E. Hossain, and M.-S. Alouini, "Analytical modeling of mode selection and power control for underlay d2d communication in cellular networks," *IEEE Trans. on Communications*, vol. 62, no. 11, pp. 4147–4161, 2014.

[15] N. Lu, T. Luan, M. Wang, X. Shen, and F. Bai, "Bounds of asymptotic performance limits of social-proximity vehicular networks," *IEEE/ACM Trans. on Networking*, vol. 22, no. 3, pp. 812–825, 2014.

[16] B. Kaufman and B. Aazhang, "Cellular networks with an overlaid device to device network," in *Proc. Asilomar Conference on Signals, Systems and Computers*, USA, 2008.

[17] T. Peng, Q. Lu, H. Wang, S. Xu, and W. Wang, "Interference avoidance mechanisms in the hybrid cellular and device-to-device systems," in *Proc. IEEE PIMRC*, Japan, 2009.

[18] X. Qu and C. G. Kang, "An effective interference alignment approach for device-to-device communication underlaying multi-cell interference network," in *Proc. IEEE ICTC*, Korea, 2012.

[19] C. Xu, L. Song, Z. Han, Q. Zhao, X. Wang, X. Cheng, and B. Jiao, "Efficiency resource allocation for device-to-device underlay communication systems: a reverse iterative combinatorial auction based approach," *IEEE J. Selected Areas in Communications*, vol. 31, no. 9, pp. 348–358, 2013.

[20] W. Sun, Y. Ge, Z. Zhang, and W.-C. Wong, "An analysis framework for inter-user interference in ieee 802.15. 6 body sensor networks: A stochastic geometry approach," *IEEE Trans. on Vehicular Technology*, to appear.

[21] R. Zhang, X. Cheng, L. Yang, and B. Jiao, "Interference-aware graph based resource sharing for device-to-device communications underlaying cellular networks," in *Proc. IEEE WCNC*, China, 2013.

[22] H. Min, J. Lee, S. Park, and D. Hong, "Capacity enhancement using an interference limited area for device-to-device uplink underlaying cellular networks," *IEEE Trans. on Wireless Communications*, vol. 10, no. 12, pp. 3995–4000, 2011.

[23] X. Chen, L. Chen, M. Zeng, X. Zhang, and D. Yang, "Downlink resource allocation for Device-to-Device communication underlaying cellular networks," in *Proceedings of IEEE PIMRC*, Australia, 2012.

[24] M. Ni, L. Zheng, F. Tong, J. Pan, and L. Cai, "A geometrical-based throughput bound analysis for device-to-device communications in cellular networks," *IEEE J. Sel. Areas Commun.*, vol. 33, no. 1, pp. 100–110, 2015.

[25] X. Lin, J. G. Andrews, and A. Ghosh, "Spectrum sharing for device-to-device communication in cellular networks," *IEEE Trans. on Wireless Communications*, vol. 13, no. 12, pp. 6727–6740, 2014.

[26] J. Liu, H. Nishiyama, N. Kato, and J. Guo, "On the outage probability of device-to-device-communication-enabled multichannel cellular networks: An rss-threshold-based perspective," *IEEE J. Selected Areas in Communications*, vol. 34, no. 1, pp. 163–175, 2016.

[27] W. Sun, E. G. Strom, F. Brannstrom, Y. Sui, and K. C. Sou, "D2d-based v2v communications with latency and reliability constraints," in *Proc. of IEEE GLOBECOM*, USA, 2014.

[28] Y. Ren, F. Liu, Z. Liu, C. Wang, and Y. Ji, "Power control in d2d-based vehicular communication networks," *IEEE Trans. on Vehicular Technology*, vol. 64, no. 12, pp. 5547–5562, 2015.

[29] S. Kostof and R. Tobias, *The city shaped*. Thames and Hudson London, 1991.

[30] G. S. Thakur, P. Hui, and A. Helmy, "Modeling and characterization of vehicular density at scale," in *Proc. IEEE INFOCOM*, Italy, 2013.

[31] M. Botsov, M. Klugel, W. Kellerer, and P. Fertl, "Location dependent resource allocation for mobile device-to-device communications," in *Proc. IEEE WCNC*, Turkey, 2014.

[32] H. ElSawy, E. Hossain, and M. Haenggi, "Stochastic geometry for modeling, analysis, and design of multi-tier and cognitive cellular wireless networks: A survey," *IEEE Communications Surveys & Tutorials*, vol. 15, no. 3, pp. 996–1019, 2013.

[33] C.-H. Yu, K. Doppler, C. B. Ribeiro, and O. Tirkkonen, "Resource sharing optimization for Device-to-Device communication underlaying cellular networks," *IEEE Trans. on Wireless Communications*, vol. 10, no. 8, pp. 2752–2763, 2011.

[34] "Tiger/line shapefiles." [Online]. Available: http://www.census.gov/geo/maps-data/data/tiger-data.html

[35] J. Härri, F. Filali, C. Bonnet, and M. Fiore, "VanetMobiSim: Generating Realistic Mobility Patterns for VANETs," in *Proc. of ACM VANET*, USA, 2006.

[36] "Winner ii channel models." [Online]. Available: http://projects.celtic-initiative.org/winner+/WINNER2-Deliverables/D1.1.2v1.1.pdf

Response to Reviewers' Comments

Journal Title: IEEE Transaction on Vehicular Technologies

Reference Number: VT-2016-00437

Title of Paper: Performance Analysis of Vehicular Device-to-Device Underlay Communication

Authors: Nan Cheng, Haibo Zhou, Lei Lei, Ning Zhang, Yi Zhou, Xuemin (Sherman) Shen, Fan Bai

We would like to take this opportunity to sincerely thank the associate editor and the reviewers for their valuable comments on our paper. We have carefully revised our manuscript taking all the comments and suggestions into consideration. The details can be found in the following responses.

I. RESPONSE TO REVIEWER 1

Thank you for the valuable comments on our paper. The responses are provided as follows, and the manuscript has been carefully revised accordingly.

Comment 1: *In the network model, what is the reason that only large-scale fading (i.e.,) path loss is considered when calculating the received power? According to the high mobility of vehicles, the small-scale fading and full CSI should also be considered, since they may have essential impacts on the results.*

Response: Due to the high mobility of vehicles, the rapid channel variations results in difficulty in obtaining real-time full CSI which contains the actual channel fading parameters. Thus, large-scale fading effects including path loss and shadowing are preferred when designing V-D2D communication protocols [1]–[3]. In addition, in [4], a simulation has been conducted, showing that the performance degradation of V-D2D communication is very little when only path loss is considered. Based on these observations, in this paper, we only consider the large-scale fading effects. Following [5] and [6], we consider a general power-law path-loss model with the decay rate $d^{-\gamma}$, where d is the distance between the transmitter and the receiver, and $\gamma > 2$ is the path-loss exponent. We have modified the manuscript accordingly.

Comment 2: *In Section III.C, a biased mode selection scheme between D2D and the cellular mode is employed. What is the main purpose and benefits of employing such a paradigm? For the most important*

parameter (bias factor), who will be in charge of calculating and deciding the value of it?

Response: The aim of the paper is to investigate the performance of V-D2D communications in a D2D underlay cellular network, which is affected by the number and locations of V-D2D users within the cellular network. Therefore, the biased channel quality based mode selection scheme is employed to model how different communication modes (cellular two-hop mode or D2D mode) are selected by cellular users. There are three main reasons for utilizing such a mode selection scheme. First, it uses a simple yet effective mode selection criterion that is tractable. The criterion is based on the comparison between the cellular channel quality ($d_C^{-\gamma_C}$) and the biased D2D channel quality ($\varphi d_D^{-\gamma_D}$). For each vehicular user, if $d_C^{-\gamma_C} > \varphi d_D^{-\gamma_D}$, cellular mode will be selected; otherwise, the D2D mode will be employed to transmit data. Due to the difference between cellular mode and D2D mode, such as cost, reliability, data rate, and delay, a bias factor φ is used to model the preference on D2D mode over cellular mode. Second, with this scheme, the interference to the cellular uplink transmissions can be controlled. A D2D transmission closer to the eNB tends to have a smaller transmission distance d_D, and a correspondingly smaller transmit power due to the channel inversion power control. Third, the biased channel quality based mode selection scheme provides a straightforward way to analyze the D2D network performance while adjusting the V-D2D user number. Adjusting the value of bias factor φ can change the preference of users on D2D mode over cellular mode, and thus changes the probability distribution of mode selection results.

The choice of bias factor φ can be determined by each user or the cellular operator, according to different concerns such as cost issues, interference control, network throughput, and so forth.

Comment 3: *The paper studies the typical grid-like street pattern, which is a common street pattern in the urban area of big cities. However, for D2D communication, it should be able to apply to other areas with cellular coverage, and different street patterns? In this way, can the analysis in the paper be extended to other street patterns?*

Response: The analysis can be easily applied to coverage patterns other than the square pattern, such as hexagon coverage, and Vorinoi coverage which is a common coverage pattern of LTE networks. The difference is that in non-regular coverage patterns such as the Vorinoi coverage, the detailed knowledge of the road segments within the coverage area, such as the lengths and locations, should be known to apply our analysis. Specifically, if such knowledge is provided, the transmit power distribution $Z_{D,i}$ and $Z_{C,i}$ can be obtained, and the power-to-interference-plus-noise ratio for each V-D2D or cellular uplink
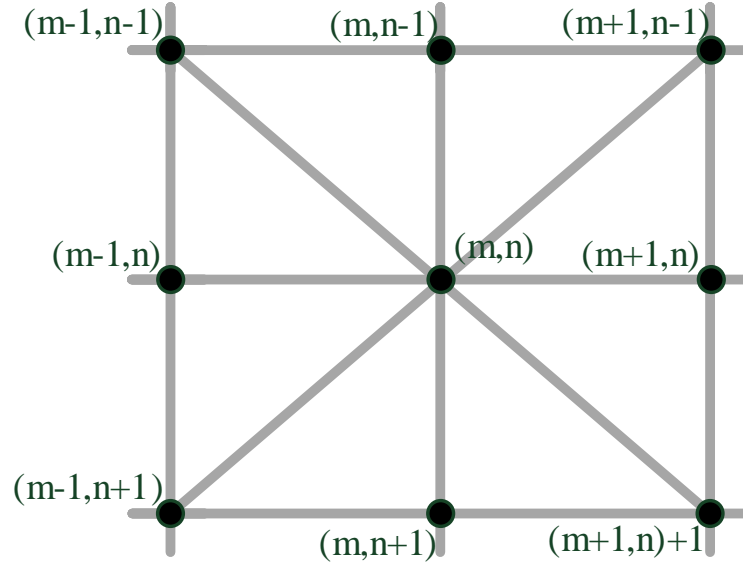
2

Fig. 1.   Random road network model.

transmission can then be calculated by (7). In addition, the grid-like street pattern can be also extended to general street patterns. According to the research in [7], a random road network model can be employed to consider the effects of obstacles and shortcuts on the road network. For an intersection (i, j), there are 8 possible paths, as shown in Fig. 2. Two probability parameters p and q are used to control the presence of horizontal/vertical road segments and diagonal road segments, respectively. By employing such a model in our analysis, the street pattern can be extended to a general case, and the performance is a function of the probability parameters p and q. We will leave the extensions to our future works.

Comment 4: *In the simulation figure 6B, for power threshold equaling -75 dBm and -80 dBm, the total throughput first increases with bias factor, and then decreases. Please explain the reason for this fact.*

Response: For the cases with $\rho_0 = -75$ dBm and $\rho_0 = -80$ dBm, the total throughput increases from $\varphi = 0.1 \times 10^{-3}$ to 0.3×10^{-3}, but decreases slightly with the further increase of φ. This is because when φ is small, the interference is low, and with the increase of φ, there are more concurrent V-D2D transmissions, leading to larger total throughput. However, when φ is relatively large, the interference becomes the dominating factor, and thus the increase of φ leads to a decrease of total throughput. For the case of $\rho_0 = -85$ dBm, the total throughput increases with φ even when φ is larger than 0.3×10^{-3}. The
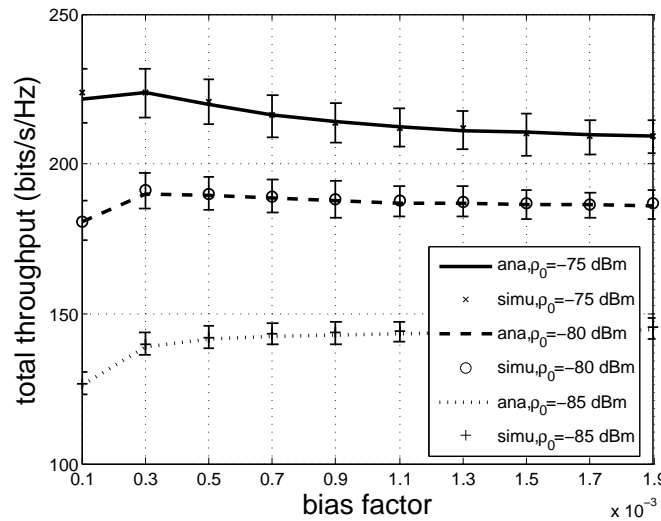
3

Fig. 2.   Fig 6b in manuscript: total throughput w.r.t. φ and ρ_0.

reason is that when ρ_0 is small, the transmit power is small according to the channel inversion model, and thus the interference is small. Therefore, as the value of φ increases, more concurrent transmissions lead to a higher throughput.

Comment 5: *Some typos and grammar errors should be corrected.*

Response: The typos and grammar errors have been corrected in the manuscript.

II. RESPONSE TO REVIEWER 2

Thank you for the valuable comments on our paper. The responses are provided as follows, and the manuscript has been revised carefully accordingly.

Comment 1 *In the abstract and introduction, the authors mention the non-homogeneous distribution of vehicle density. However, in the following parts of the paper, this point is not discussed again. Could the author clarify the impacts of the non-homogeneous vehicle distribution? Personally, I think the non-homogeneous vehicle distribution may influence both equation (1) and (2).*

Response: In the urban areas, the vehicle density is affected by many factors, and therefore not homogeneous in different locations and at different times. In [8], Thakur *et. al* investigated the vehicle density of over 800 locations from six large cities around the world. It is shown that the vehicle density changes with the time and location. This spatial and temporal variance in vehicle traffic density is due to many reasons, such as social spots (shopping malls, office buildings, parking lots) which is more related to people's social life [9] and peak hours when the traffic to/from work places is heavy [10]. Though,

4

in [8], the authors also found that the vehicle density in a location can be well modeled by heavy-tail distributions, such as log-gamma distribution and Weibull distribution.

In the paper, we consider that non-homogeneous vehicle density in the city. When consider at a given time and a certain location (denoted by road segment r_i), the vehicle number in r_i can be represented by ϵ_i, with PDF $f_{\epsilon,i}(x)$ and CDF $F_{\epsilon,i}(x)$, respectively. In this way, the vehicle density ϵ_i will affect $p_{T,i}$, which is the probability of a transmission request happening in road segment r_i, and can be calculated by $p_{T,i} = 1 - F_{\epsilon,i}(2)$. $p_{T,i}$ will further impact the aggregate SINR

$$\eta_i = \frac{\rho_0 h}{n_0 + \sum_{r_j \in \mathcal{M}_\mathcal{I} \backslash r_i} \mathbb{1}_{D,j} Z_{D,j} h d_{ji}^{-\gamma_D} + \mathbb{1}_{C,j} Z_{C,j} h d_{j0}^{-\gamma_C}}, \tag{1}$$

where $\mathbb{P}(\mathbb{1}_{D,i} = 1) = p_{T,i} p_{D,i}$, and $\mathbb{P}(\mathbb{1}_{C,i} = 1) \approx \frac{p_{T,i}(1-p_{D,i})}{\sum_{r_i \in \mathcal{M}_\mathcal{C}} p_{T,i}(1-p_{D,i})}$. This means that the interference is generated from a road segment r_i only if there is D2D or cellular transmission in that road segment. Then, the system performance SINR outage probability and spectrum efficiency is affected by the vehicle density.

Comment 2 *the authors state that without the loss of generality, V-D2D transmissions can happen only when two VUEs are in the same road segment. It may be better to consider this statement as an assumption and this assumption does loses some generality of the practical system.*

Response: As suggested, the statement "V-D2D transmissions can happen only when two VUEs are in the same road segment" is more suitable to be an assumption since the analysis of the paper cannot be simply applied to other cases. Therefore, we assume that in the considered V-D2D underlaying cellular network, the V-D2D transmissions can happen when the two VUE are in the same road segment r_i, and justify the assumption. V-D2D transmissions are only available for vehicles in proximity, and it is usually difficult for the signal to transmit between two intersected road segments in urban areas due to the block of buildings. In addition, vehicles in the same road segment are more likely to preserve a longer and more reliable connection, which avoids frequent D2D connection set up and tear down. Therefore, it is reasonable to assume that the eNB can schedule V-D2D communication only when two VUEs are within one road segment. A similar assumption can be found in [9]. We have revised the manuscript accordingly.

Comment 3 *the authors state that $d_{C,i}$ is approximated by the distance from the eNB to the middle point of r_i. This approximation could be good for far-away road segments. However for nearby road segments, it may not model the system well because the interference from nearby vehicles may influence*

the system significantly. Could the author model the far-away and nearby area separately or find some supporting arguments for such approximation?

Response: When analyzing the scenario where the road segment r_i is close enough to the eNB, such an approximation is no further suitable. In this case, the distribution of D2D transmission distance d_D (we consider the road segment r_i and thereafter the index i is ignored) is related to the locations of VUEs. As shown in Fig. 3(a), consider r_i starts at point 0 and ends at point L, and one VUE (assuming transmitting VUE) is located at point x. Next, we derive the distribution of d_D conditioned on x, $f_D(d_D|x)$. From the figure, we can easily obtain that for $x < \frac{L}{2}$, we have

$$f_{D|x}(d_D|x) = \begin{cases} \frac{2x}{L}, & d_D < x \\ 1 - \frac{2x}{L}, & \text{otherwise} \end{cases} \tag{2}$$

and for $x \geq \frac{L}{2}$, $f_{D|x}(d_D|x) = f_{D|x}(d_D|L - x)$. Note that given x, the cellular transmission distance d_C can be easily calculated. Then, we can derive the probability of mode selection results given x. Denote by $p_{D|x}$ the probability of selecting D2D mode given x. According to the biased channel quality mode selection, $p_{D|x}$ can be calculated by

$$p_{D|x} = \mathbb{P}(\varphi d_{D|x}^{-\gamma_D} \geq d_{C|x}^{-\gamma_C})$$
$$= F_{D|x}(\varphi^{\frac{1}{\gamma_D}} d_C^{\frac{\gamma_C}{\gamma_D}} |x), \tag{3}$$

where $F_{D|x}(d|x)$ is the cumulative distribution function (CDF) of d_D conditioned on x. Then, from Fig. 3(b), we can easily obtain the value of $p_{D|x}$. To analyze the network performance, it is required to obtain the unconditioned mode selection probability p_D, which can be calculated by

$$p_D = \int_0^L p_{D|x} f(x) dx, \tag{4}$$

where $f(x) = \frac{1}{L}$. Obtaining p_D, we will be able to analyze the SINR and network performance following the methods in the manuscript.

In addition, it is worth to note that to analyze the overall network performance, the approximation of $d_{C,i}$ by the distance from the eNB to the middle point of r_i is sufficient and simple. Due to the mode selection scheme, it is more unlikely for a VUE to choose D2D mode with a smaller distance from the VUE to the eNB. And since only one cellular mode VUE can be scheduled, the "inner area" (small area
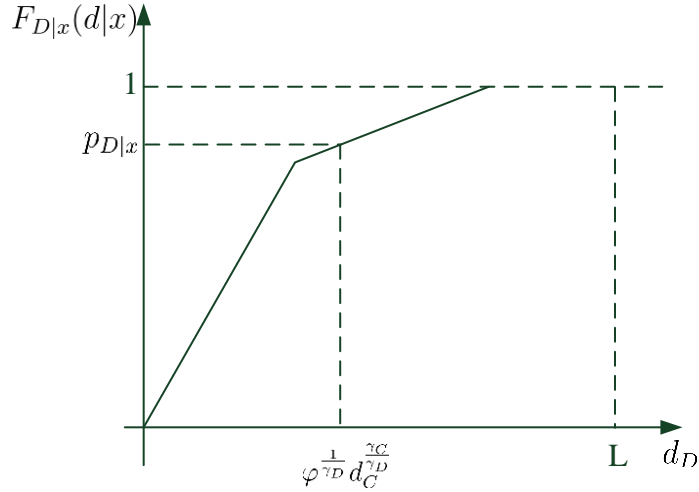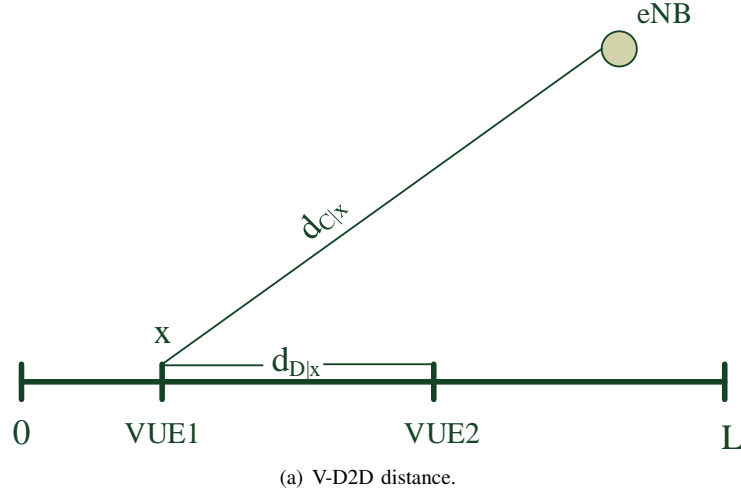
6

(a) V-D2D distance.

(b) Calculate $p_{D|x}$.

Fig. 3.   Calculate p_D using exact d_C.

around the eNB) has less impact on the network performance than the "outer area". This can be validated by the simulation in which the exact d_C is employed other than a proximate one. We can see that in simulation figures, the analyzed results match the simulation results well. Moreover, in practice, the two VUEs in a V-D2D pair often mutually transmit, and therefore it is difficult to determine d_C. In this way, a proper approximation of d_C is needed.

Comment 4 *the author states in the considered urban V-D2D scenario, power truncate outage does not happen since P_m is large enough. This statement is based on the assumption that the cellular and D2D have similar path loss exponents, i.e., γ_C and γ_D. In the simulation part, the authors also adopt the parameters $\gamma_C = \gamma_D = 4$, are there any arguments for such parameter settings?*

7

Response: According to [11], the typical form of path-loss model can be written as

$$PL[dB] = A \log_{10}(d[m]) + B + C \log_{10}(\frac{f_c[GHz]}{5.0}) + X, \tag{5}$$

where $PL[dB]$ is the path-loss in dB, $d[m]$ is the distance between the transmitter and the receiver in meters, and $f_c[GHz]$ is the system frequency in GHz. Among the three parameters A, B, and C, A is related to the path-loss exponent γ, where $\gamma = \frac{A}{10}$, B is the intercept, C represents the frequency-dependent part of path loss, and X is the environment-specific term. Since in the paper, we employ the power-law path-loss model, we then focus on the path-loss exponent γ.

For γ_C, i.e., the path-loss exponent for cellular transmissions, according to [11], γ_C can be taken as the path-loss in "urban macro cell" scenario. For this scenario, γ_C can be expressed by

$$PL[dB] = 40 \log_{10}(d) + 13.47 + 6.0 \log_{10}(\frac{f_c}{5.0}) - 14.0 \log_{10}(h'_{BS}) - 14.0 \log_{10}(h'_{MS}), \tag{6}$$

where h'_{BS} and h'_{MS} are the heights of the base station and mobile station, respectively. From (6), it is clear that $\gamma_C = 4$. For γ_D, i.e., the path-loss exponent for V-D2D transmissions, we can still use (6). However, due to the commonly short communication distances, it is more proper to apply the "urban micro cell" scenario, where the path-loss can be expressed by

$$PL[dB] = 40 \log_{10}(d) + 9.45 + 2.7 \log_{10}(\frac{f_c}{5.0}) - 17.3 \log_{10}(h'_{BS}) - 17.3 \log_{10}(h'_{MS}). \tag{7}$$

Therefore, we can know that for urban scenarios, $\gamma_C = \gamma_D = 4$ is a reasonable setting. We have revised the manuscript accordingly.

Comment 5 *The authors evaluate some performance metrics of D2D communication and cellular uplink communication (first hop of vehicle-to-vehicle communication through cellular network). However, the paper tries to compare the performance of vehicle-to-vehicle data service. Should the second hop (downlink) communication of the cellular network be included and will it make make any difference?*

Response: As the reviewer mentioned, the performance of vehicle-to-vehicle data service via cellular transmission should consider both hops ,i.e., uplink (transmitting VUE to eNB) performance and downlink (eNB to receiving VUE) performance. According to [5], since the end-to-end performance is determined by the bottleneck link which is the cellular uplink, the end-to-end rate can be roughly estimated by $0.5R_{c,u}$, where $R_{c,u}$ is the uplink data rate. Therefore, in our paper, we first derive the cellular uplink performance.

8

And if the vehicle-to-vehicle data service performance is considered, we can follow the same consideration and estimate it by half of the cellular uplink rate.

Comment 6 *Some typos, e.g., in the paragraph above equation (7), for the sentence with the total interference $\mathcal{I}_i$ given in (7), should the (7) be (6); in the figures, ϕ and φ are mixed together.*

Response: We have carefully revised the manuscript.

III. RESPONSE TO REVIEWER 3

Thank you for the valuable comments on our paper. The responses are provided as follows, and the manuscript has been revised carefully accordingly.

Comment 1 *However, the assumed scenario is not so realistic by considering equal size street blocks. The simulations are also run in the assumed scenario, which cuts into the value. The comparison between realistic scenario and the assumed scenario is not studied or discussed in the analysis and simulation part. The reviewer suggests the authors may compare the analytical results with that in some realistic applications in the simulation part.*

Comment 2 *It would be helpful to discuss how to extend the results in this paper in the grid topology to other coverage patterns such as hexagon and Vorinoi coverage.*

Response to comments 1 and 2: The analytical results obtained in the paper are not limited to the grid-like street pattern and square cellular coverage area. Here we show how the results are easily extended to other scenarios where the street patterns are irregular, and the cellular coverage is more general, such as hexagon and Vorinoi coverage, provided that the geographic information and vehicle density of each road segment is known.

Consider an urban area with a set of road segment $\mathbf{r} = \{r_1, r_2, \ldots, r_W\}$. For each road segment r_i, the geographic information such as the locations of end points is known. This information can be obtained from geo-location databases such as TIGER/Line Shapefiles [12]. The vehicle density in r_i is denoted by ϵ_i, with the PDF and CDF denoted by $f_{\epsilon,i}(x)$ and $F_{\epsilon,i}(x)$, respectively. Consider a cellular coverage area Ω_C, the set of road segment $\mathbf{r}$ is divided into two subsets, $\mathbf{r_c}$ the set of road segments within Ω_C, and $\bar{\mathbf{r_c}}$ the set of road segments outside Ω_C. Then, we can calculate the SINR of uplink/D2D transmissions in road segment $r_i \in \mathbf{r_c}$ by

$$\eta_i = \frac{\rho_0 h}{n_0 + \sum_{r_j \in \mathbf{r} \backslash r_i} \mathbb{1}_{D,j} Z_{D,j} h d_{ji}^{-\gamma_D} + \mathbb{1}_{C,j} Z_{C,j} h d_{j0}^{-\gamma_C}}, \tag{8}$$
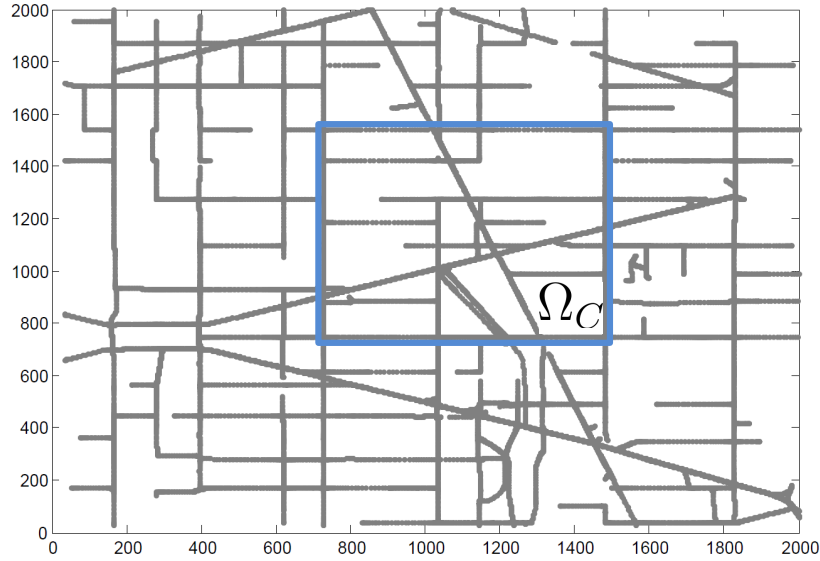
9

Fig. 4.   Simulation in realistic scenario: a 2.0 km × 2.0 km region road map of the downtown area of Washinton D.C.

where d_{ji} and d_{j0} can be calculated from the geographic information of road segments. With SINR obtained, the performance metrics such as SINR outage probability and spectrum efficiency can be then theoretically analyzed, similar to the methods in the paper.
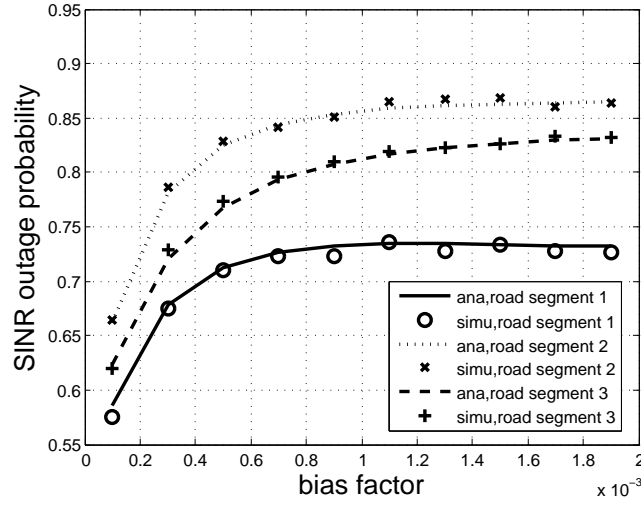
To validate the extension, we conduct simulation in a 2.0 km × 2.0 km region road map of the downtown area of Washinton D.C. Each street segment has two lanes with the bidirectional vehicle traffic. We use VANETMobisim [13] to generate the mobilities of 300 vehicles. Speed limit is set to 50 km/h. The vehicle mobility is controlled by Intelligent Driver Model with Lane Changes (IDMLC) model, in which vehicle speed is based on movements of vehicles in neighborhood. We then simulate the network performance of the cellular network with the coverage areas Ω_C as shown in Fig. 4. To show that the analytical method used in the paper can be easily and accurately extended, the comparison of simulation and theoretical results of different road segments is plotted in Fig. 5. From the figures, we can see that the analytical results and simulation results match well for different road segments, which validates the feasibility of the extension of the analytical method to realistic scenarios.

Comment 3 *As the derived outage probability and throughput are completed, please discuss the traceability of the expressions.*

Response: In this paper, we have derived the expression of the SINR outage probability and throughput
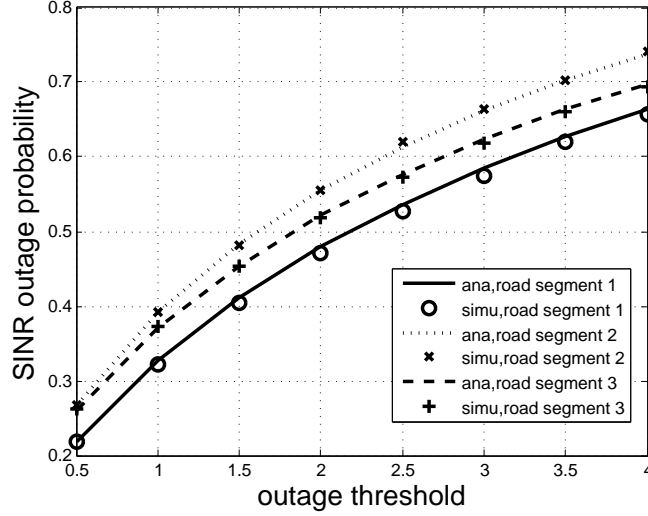
(a) SINR outage probability w.r.t. ω.

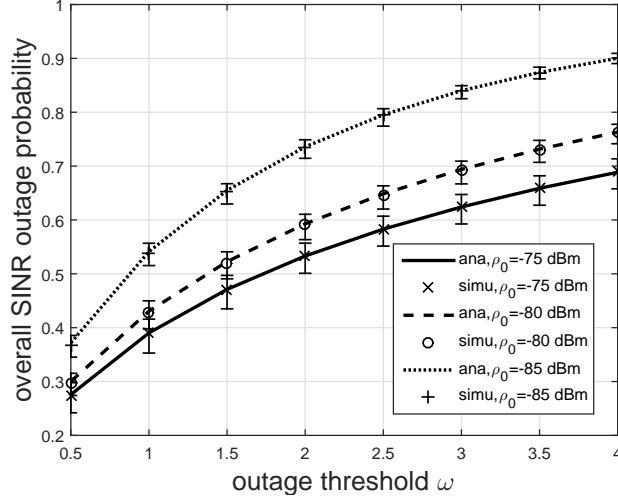(b) SINR outage probability w.r.t. φ.

Fig. 5.   Simulation in real map scenario.

(spectrum efficiency) as

$$p_{o,i}(\omega) = \mathbb{P}(\eta_i \leq \omega) \stackrel{ii}{=} 1 - \exp\{-\frac{\omega n_0}{\rho_0}\}\mathcal{L}_{\mathcal{D},i}(\frac{\omega}{\rho_0})\mathcal{L}_{\mathcal{C},i}(\frac{\omega}{\rho_0}), \tag{9}$$

and

$$\sigma_i = \mathbb{E}[\log_2(1 + SINR_i)] = \int_0^\infty 1 - p_{o,i}(2^x - 1)dx, \tag{10}$$

respectively. To validate the traceability of the expressions, we have conducted simulations, and compare the simulation results and the theoretical results obtained from (9) and (10), while varying key design parameters, i.e., bias factor φ, receive power threshold ρ_0, and the SINR outage threshold ω. The com-

11

(a) Varied channel inversion threshold ρ_0.
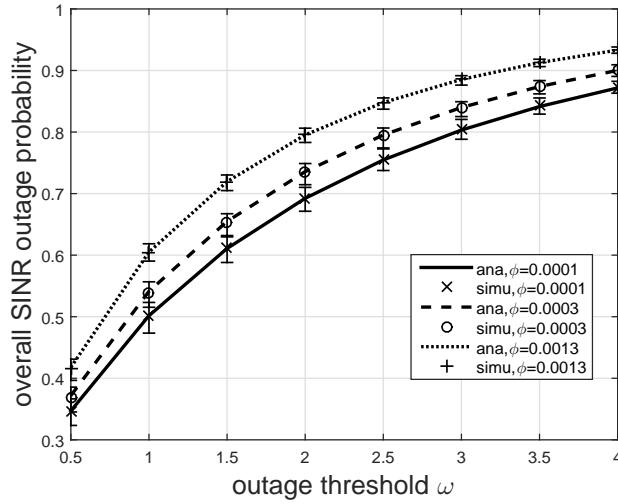
(b) Varied bias factor φ.

Fig. 6.　SINR outage probability w.r.t. ω.

parison of simulation and theoretical results are plotted in Fig. 6 to Fig. 8 with 90% confidence intervals. From the figures, we can see that with different combinations of the design parameters φ, ρ_0, and ω, the simulation results and theoretical results match each other well, either for SINR outage probability and throughput, which indicates that the expression obtained in this paper is well traceable. We have revised the manuscript accordingly.

Comment 4 *The references are not sufficient. Please add more relevant literatures in D2D communication and performance analysis, such as*

1. Device-to-Device Communication in LTE-Advanced Networks: A Survey

2. On the Outage Probability of Device-to-Device Communication Enabled Multi-Channel Cellular Net-
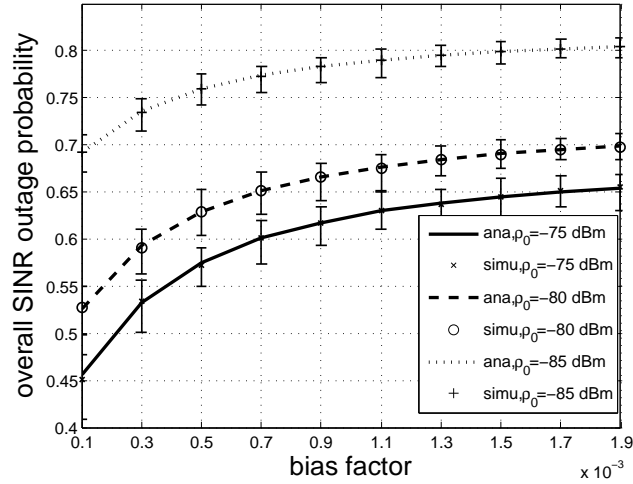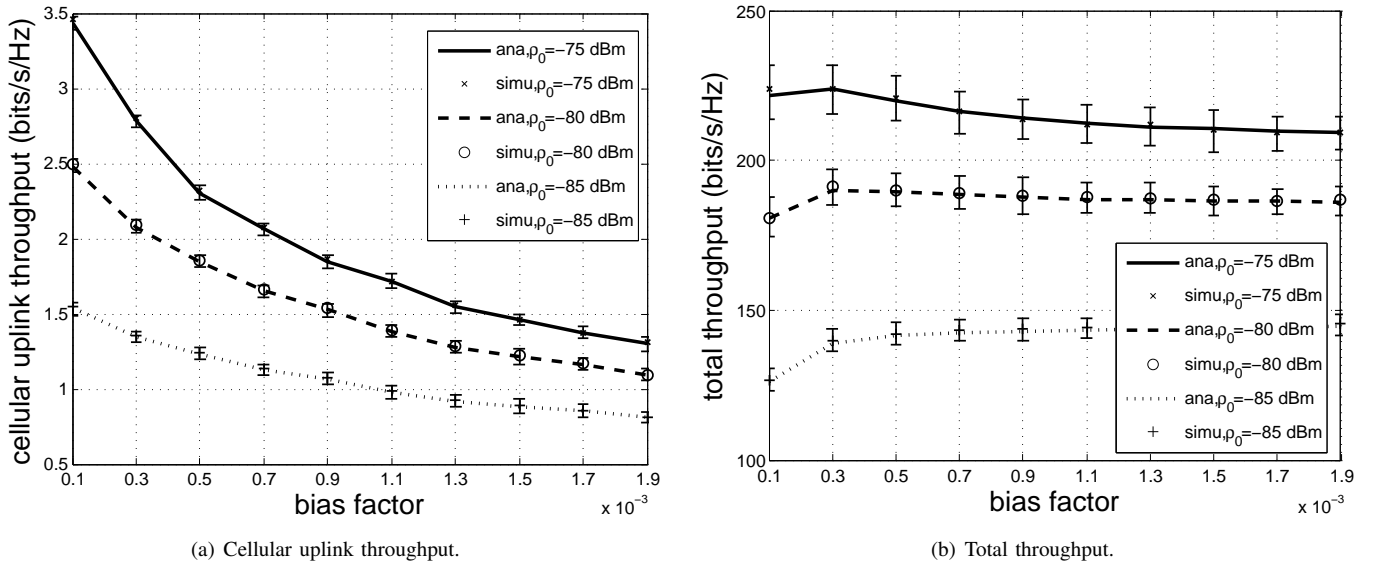
12

Fig. 7.   SINR outage probability w.r.t. φ.

(a) Cellular uplink throughput.

(b) Total throughput.

Fig. 8.   Throughput performance w.r.t. φ.

works: A RSS Threshold-Based Perspective

3. An Analysis Framework for Inter-user Interference in IEEE 802.15.6 Body Sensor Networks: A Stochastic Geometry Approach

4. Device-to-Device Communications Achieve Efficient Load Balancing in LTE-Advanced Networks

Response: The reference has been updated with additional valuable references cited [14]–[17].

REFERENCES

[1] W. Sun, E. G. Strom, F. Brannstrom, Y. Sui, and K. C. Sou, "D2d-based v2v communications with latency and reliability constraints," in *Proc. of IEEE GLOBECOM*, USA, 2014.

13

[2] M. Botsov, M. Klugel, W. Kellerer, and P. Fertl, "Location dependent resource allocation for mobile device-to-device communications," in *Proc. IEEE WCNC*, Turkey, 2014.

[3] Y. Ren, F. Liu, Z. Liu, C. Wang, and Y. Ji, "Power control in d2d-based vehicular communication networks," *IEEE Trans. on Vehicular Technology*, vol. 64, no. 12, pp. 5547–5562, 2015.

[4] X. Cheng, L. Yang, and X. Shen, "D2D for intelligent transportation systems: A feasibility study," *IEEE Trans. on Intelligent Transportation Systems*, to appear.

[5] H. ElSawy, E. Hossain, and M.-S. Alouini, "Analytical modeling of mode selection and power control for underlay d2d communication in cellular networks," *IEEE Trans. on Communications*, vol. 62, no. 11, pp. 4147–4161, 2014.

[6] C. Xu, L. Song, Z. Han, Q. Zhao, X. Wang, X. Cheng, and B. Jiao, "Efficiency resource allocation for device-to-device underlay communication systems: a reverse iterative combinatorial auction based approach," *IEEE J. Selected Areas in Communications*, vol. 31, no. 9, pp. 348–358, 2013.

[7] W. Peng, G. Dong, K. Yang, and J. Su, "A random road network model and its effects on topological characteristics of mobile delay-tolerant networks," *IEEE Trans. on Mobile Computing*, vol. 13, no. 12, pp. 2706–2718, 2014.

[8] G. S. Thakur, P. Hui, and A. Helmy, "Modeling and characterization of vehicular density at scale," in *Proc. IEEE INFOCOM*, Italy, 2013.

[9] N. Lu, T. Luan, M. Wang, X. Shen, and F. Bai, "Bounds of asymptotic performance limits of social-proximity vehicular networks," *IEEE/ACM Trans. on Networking*, vol. 22, no. 3, pp. 812–825, 2014.

[10] S. Uppoor and M. Fiore, "Characterizing pervasive vehicular access to the cellular ran infrastructure: an urban case study," *IEEE Trans. on Vehicular Technology*, vol. 64, no. 6, pp. 2603–2614, 2015.

[11] "Winner ii channel models." [Online]. Available: http://projects.celtic-initiative.org/winner+/WINNER2-Deliverables/D1.1.2v1.1.pdf

[12] "Tiger/line shapefiles." [Online]. Available: http://www.census.gov/geo/maps-data/data/tiger-data.html

[13] J. Härri, F. Filali, C. Bonnet, and M. Fiore, "VanetMobiSim: Generating Realistic Mobility Patterns for VANETs," in *Proc. of ACM VANET*, USA, 2006.

[14] J. Liu, N. Kato, J. Ma, and N. Kadowaki, "Device-to-device communication in lte-advanced networks: a survey," *IEEE Communications Surveys & Tutorials*, vol. 17, no. 4, pp. 1923–1940, 2014.

[15] J. Liu, H. Nishiyama, N. Kato, and J. Guo, "On the outage probability of device-to-device-communication-enabled multichannel cellular networks: An rss-threshold-based perspective," *IEEE J. Selected Areas in Communications*, vol. 34, no. 1, pp. 163–175, 2016.

[16] W. Sun, Y. Ge, Z. Zhang, and W.-C. Wong, "An analysis framework for inter-user interference in ieee 802.15. 6 body sensor networks: A stochastic geometry approach," *IEEE Trans. on Vehicular Technology*, to appear.

[17] J. Liu, Y. Kawamoto, H. Nishiyama, N. Kato, and N. Kadowaki, "Device-to-device communications achieve efficient load balancing in lte-advanced networks," *IEEE Wireless Communications*, vol. 21, no. 2, pp. 57–65, 2014.